NASA. TM-X- 72597

NSSDC
WDC-A-R&S

76-04

National Space Science Data Center/
World Data Center A For Rockets and Satellites

(NASA-TM-X-72597) AE 6: A MODEL ENVIRONMENT OF TRAPPED ELECTRONS FOR SOLAR MAXIMUM (NASA) 67 p HC $4.50 CSCL 03B

N76-23139

Unclas
G3/92 27822

AE 6: A Model Environment of Trapped Electrons for Solar Maximum

May 1976

NSSDC/WDC-A-R&S 76-04

AE 6: A Model Environment of Trapped Electrons for Solar Maximum

by

Michael J. Teague
King W. Chan
James I. Vette

May 1976

National Space Science Data Center
National Aeronautics and Space Administration
Goddard Space Flight Center
Greenbelt, Maryland 20771

CONTENTS

TABLE

ILLUSTRATIONS

ILLUSTRATIONS (continued)

ILLUSTRATIONS (concluded)

Note: The abbreviations "L LE" and "L GE," appearing in this list and on the figures, mean "L is less than or equal to" and "L is greater than or equal to," respectively. For the abbreviation "L equals," a blank space follows the letter "L." The symbols ≤ for LE, ≥ for GE, and = for equals appear in the text.

I. INTRODUCTION

This report presents a projected inner zone electron model environment, AE 6, for the epoch 1980. It is intended to provide estimates of mission fluxes that spacecraft will encounter in the coming solar maximum years.

In the previous solar maximum model, AE 5,[1] for the epoch 1967, the inner zone electron fluxes contained a substantial contribution from the Starfish event of July 1962. These artificial electron fluxes continuously decayed and then became insignificant in the environment after 1970.[2] Therefore, the necessity arises to construct the inner zone model which gives the solar maximum projection of the radiation environment after the removal of Starfish electrons. The solar maximum environment for the outer zone has been presented by the model AE 4.[3]

AE 6 is presented by graphs of omnidirectional integral flux as a function of L shell, the ambient magnetic field B, and the energy E. Results of orbital integrations for altitudes from 150 n.m. to 18,000 n.m. are given for circular orbits with four different inclinations, using the AE 6 and the AE 4 solar maximum models for the inner and outer zones, respectively.

Section III describes the derivation of AE 6 and gives a brief comparison of the radial profiles of equatorial fluxes from several related models. The appendix following Section III contains a short summary of the associated computer programs.

II. THE SOLAR MAXIMUM ENVIRONMENT - FLUX MAPS

To make estimates for mission fluxes, useful maps of the spatial distribution and energy dependence of the radiation environment in the magnetosphere can be constructed by using coordinates B and L.[4] The present electron omnidirectional integral flux model covers threshold energies E from 40 kev to 4 Mev and L shells from 1.2 to 11.0 Earth radii.

Nomographs are used to present two groups of flux maps. The first group, Figures 1 through 9, shows electron fluxes as a function of L, B, and E. The second group, Figures 10 through 17, gives the orbit-integrated fluxes as a function of orbital altitude (n.m.) and inclination (deg). This application of the nomograph was called "carpet plot" and has been documented.[1]

There are three carpet plots mapping each of the threshold energies (E = .04, .1, .25, .5, .75, 1.0, 2.0, 3.0, and 4.0 Mev). The first carpet plot, A, covers the inner zone; the second carpet plot, B, depicts the slot region; and the third carpet plot, C, extends to the outside edge of the outer zone. Thus, a complete spatial coverage of the two radiation belts for the nine threshold energies is provided by 27 carpet plots in Figures 1 through 9, each figure consisting of three carpet plots: A, B, and C.

It is noted that outer zone fluxes ($L \geq 3.0$) are generated from the AE 4 1967 model. This model contains a description of the temporal variations of the electron fluxes and the dependence on local time.[3] The model used for the type of average required for orbit integrations is based on an average over both of these fluctuations.

The carpet plots of the slot region, Plot B of each threshold energy, contain the interfaces of the inner zone and outer zone models. It is noted that the transitions between L = 2.6 to L = 3.0 are quite smooth at low B values (equatorial region), but not at high B values. This is the result of the different B dependence used in the independent modeling of inner zone and outer zone. The B dependence of the AE 6 model is the same as AE 5, which is quite different from AE 4.[5]

Carpet plots of orbit-integrated fluxes appear in Figures 10 through 17. The fluxes accumulated per day by "flying" in the circular orbits of a given inclination are plotted as a function of orbital altitudes and threshold energies. The computation is based on the AE 6 and AE 4 solar maximum model environments, using the program ORP (Appendix). Data have been generated for the circular orbits at four inclinations: 0, 30, 60, and 90 deg. Each of these orbital integration carpet plots covers altitudes ranging either from 150 to 4,000 n.m. or from 4,500 to 18,000 n.m. for a given inclination. The observation of no significant flux in the 0-deg inclination orbit at the low altitude of 150 n.m. is attributed to the fact that low-altitude fluxes are encountered only in the South Atlantic Anomaly and that this region does not extend to 0-deg latitude.

Other useful categories of graphic model presentation are the iso-flux maps in B-L and R-λ coordinates, where R and λ are radial distance in Earth radii and magnetic latitude in deg, respectively. Figures 18 through 23 are the iso-flux contour maps for threshold energies 40 kev, 500 kev, and 1 Mev. These maps are shown for the AE 6 model only. Corresponding outer zone maps have been published.[3]

III. MODEL DERIVATION AND COMPARISON

Unlike the previous electron model, AE 5 1967, AE 6 is not directly constructed from in situ measurements. It is derived from the corrected AE 5 1967 model in conjunction with a Starfish model.[2] The derivation is designed to obtain a projection of the solar maximum environment after removing the artificial electrons.

The model AE 5 is based on data from five satellites: OGO 1, OGO 3, 1963-38C, OV3-3, and Explorer 26, spanning the period September 1964 to December 1967. For the model epoch 1967, the model is designated as AE 5 1967 to represent the solar maximum condition with a significant Starfish contribution.

Subsequent to the derivation of the AE 5 1967 model, the reported value for the efficiency of the OV3-3 spectrometer was increased by a factor of four. As a result, the flux levels in the data were reduced by the same factor. The required corrections and adjustments in the model fluxes have been described in detail in an earlier publication.[6]

Generally, the efficiency change of OV3-3 data affects the AE 5 model for all energies above 250 kev. The effect, however, is more pronounced for E > 700 kev and L > 1.6 Earth radii because OV3-3 data were the only measurements used by the model for these energies in that region. Figure 24 is a block diagram showing the changes made for the derivation of the new model, AE 6, as a function of energy and L shell.

The subtraction of residual Starfish fluxes from model AE 5 1967 is based on a previously documented study of the Starfish electron decay.[2] The decay-time contours and the cutoff-time contours derived in that

study have been used to estimate the artificial electron residual in the AE 5 1967 model. The quantitative details are obtained from Table 2 and Figures 9 and 24 of that document. It has been shown that no Starfish residual electrons for energies less than 250 kev were observed after September 1964. Hence, no adjustment is made for $E < 250$ kev in the AE 6 model.

The previously discussed Starfish model was developed by using the data from eight satellites: OGO 1, OGO 3, 1963-38C, OV1-2, Pegasus-A, Pegasus-B, Explorer 15, and Explorer 26. Assuming a linear formulation with exponential time decay, the polynomial coefficients, cutoff time, and decay time of the artificial electrons were determined by various iterative procedures. In light of the substantial differences in several decay-time measurements (i.e., references 7, 8, and 9), an average decay-time profile was obtained. These results were used to account for the probable long-term effects of the artificial electron decay. Estimates of the uncertainty factors appear in the same document.[2]

The effects of the OV3-3 efficiency change in the AE 5 1967 model and of the removal of Starfish flux in the inner zone are shown by the radial profiles given in Figures 25 through 30. In addition to the solar maximum model environments, the projected solar minimum model AE 5 1975 profiles[6] are given in each figure for comparison. The OV3-3 efficiency change was most important for the higher energy regions and is seen most clearly in Figures 28 through 30. The Starfish decay was most important for L values in the range 1.2 to 1.7 and energies greater than 500 kev.

There is little difference between the solar maximum and solar minimum models at high energies and low L values. However, as shown in Figures 25, 26, and 27, the dependence of electron flux on the solar cycle becomes more pronounced for energies below 250 kev. At these energies very little modification was made for the Starfish flux subtraction. For L values greater than 1.6 and energies less than 1 Mev, the differences between solar maximum and solar minimum become quite large.

In Figures 31 and 32, equatorial radial profiles in the interface region between AE 6 and the AE 4 solar maximum model are presented for threshold energies of .04, .25, .5, 1.0, 2.0, 3.0, and 4.0 Mev. For L values between 2.4 and 3.0 Earth radii, a smoothing interpolation procedure has been applied to the model boundaries to produce continuous and smooth radial profiles.

Since the AE 6 model is derived from AE 5, the accuracy of the new model is limited by that of AE 5. Estimates of confidence codes for various L and E ranges of AE 6 are listed in Table 1. For regions and energies with no significant flux adjustments, the same confidence codes as in the AE 5 document[6] are adopted. In areas that required substantial Starfish flux subtraction, the AE 5 codes have been downgraded. Within these limits of accuracy, the AE 6 model presented in this report should serve the purpose of a reference of environment projection.

APPENDIX

Computer Programs MODEL and ORP

Programs MODEL and ORP have been modified to accommodate the new electron and proton models, AE 6 and AP 8.[10] Version 3.0 of these programs is described in this appendix and replaces Version 1.0[11] and Version 2.0.[6]

The current models issued by NSSDC are for solar minimum electrons AE 4 1964 (AE4MIN) and AE 5 1975 projected (AE5MIN), for solar maximum electrons AE 4 1967 (AE4) and AE 6 1980 (AE6MAX), for solar minimum protons AP 8 1964 (AP8MIN), and for solar maximum protons AP 8 1970 (AP8MAX). The models being used are stored in common blocks that are referenced by the program. In program MODEL the COMMON statements for these blocks are included in subroutine TYPE, and in ORP they are included in MAIN.

On page 15 of "The Use of the Inner Zone Electron Model AE-5 and Associated Computer Programs,"[11] the variable MTYPE in Column 9 of Card "a" for program MODEL has the following values in Version 3.0:

MTYPE	Model Used
1	AP8MAX
2	AP8MIN
3	AE6MAX for $L \leq 2.8$, AE4 for $L > 2.8$
4	AE5MIN for $L \leq 2.8$, AE4MIN for $L > 2.8$

On page 24 of that document, the variable MODEL in Column 70 of Card "a" has the following values in Version 3.0:

MODEL	Model Used
1	AP8MAX
2	AP8MIN
3	AE6MAX for L ≤ 2.8, AE4 for L > 2.8
4	AE5MIN for L ≤ 2.8, AE4MIN for L > 2.8

REFERENCES

1. Teague, M. J., and J. I. Vette, "The Inner Zone Electron Model AE 5," NSSDC 72-10, November 1972.

2. Teague, M. J., and E. G. Stassinopoulos, "A Model of the Starfish Flux in the Inner Radiation Zone," GSFC X-601-72-487, December 1972.

3. Singley, G. W., and J. I. Vette, "A Model Environment for Outer Zone Electrons," NSSDC 72-13, December 1972.

4. Roederer, J. G., "Dynamics of Geomagnetically Trapped Radiation," Berlin-Heidelberg-New York, Springer-Verlag, 1970.

5. Hilberg, R. H., M. J. Teague, and J. I. Vette, "Comparison of the Trapped Electron Models AE-4 and AE-5 with AE-2 and AE-3," NSSDC 74-13, September 1974.

6. Teague, M. J., and J. I. Vette, "A Model of the Trapped Electron Population for Solar Minimum," NSSDC 74-03, April 1974.

7. Rosen, A., and N. L. Sanders, "Loss and Replenishment of Electrons in the Inner Radiation Zone during 1965-1967," J. Geophys. Res., 76(1), 110-121, 1971.

8. Farley, T. A., "Radial Diffusion of Starfish Electrons," J. Geophys. Res., 74(14), 3591-3600, 1969.

9. Stassinopoulos, E. G., and P. Verzariu, "General Formula for Decay Lifetimes of Starfish Electrons," J. Geophys. Res., 76(7), 1841-1844, 1971.

10. Sawyer, D. M., and J. I. Vette, "Trapped Proton Environment for Solar Maximum and Solar Minimum," NSSDC/WDC-A-R&S 76-06, to be published.

11. Teague, M. J., J. Stein, and J. I. Vette, "The Use of the Inner Zone Electron Model AE-5 and Associated Computer Programs," NSSDC 72-11, November 1972.

Table 1. Omnidirectional Flux Confidence Codes for AE 6

Code	L Range	E Range	Comments
1	<1.25	≥3 Mev	Extrapolation on B, L, and E
3	≥1.3	≥3 Mev	Extrapolation on E and B
5	1.3-1.6	.7-3 Mev	Starfish model used to estimate artificial flux
5	1.9-2.4	>250 kev	Storm effects. Corrected for OV3-3 data
6	1.6-1.9	.7-3 Mev	Minor adjustment for Starfish flux
6	1.9-2.4	<250 kev	Some storm effect
9	1.3-1.9	250-700 kev	Minor modification with spect to AE 5 1967
10	1.3-1.9	<250 kev	Same as AE 5 1967

Code	Model Accuracy
10	Factor of 2
1	Order of Magnitude

FIGURE 1A OMNIDIRECTIONAL INTEGRAL FLUX MAP

40 KEV ELECTRONS FOR L LE 2.4

MODEL AE6 SOLAR MAXIMUM PROJECTED

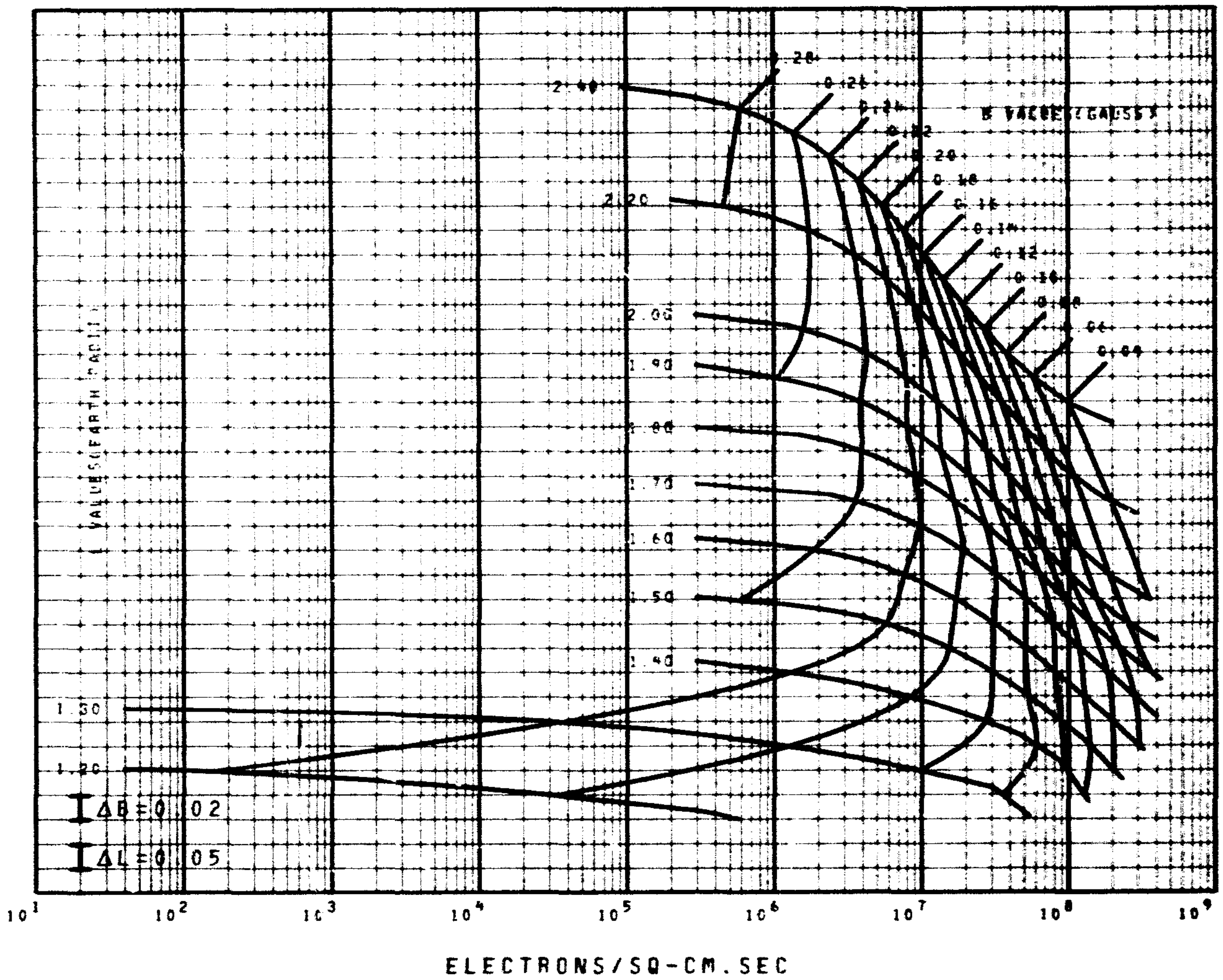

FIGURE 1B OMNIDIRECTIONAL INTEGRAL FLUX MAP

40 KEV ELECTRONS FOR L 2.6 TO 6.0

MODEL AE4 SOLAR MAXIMUM

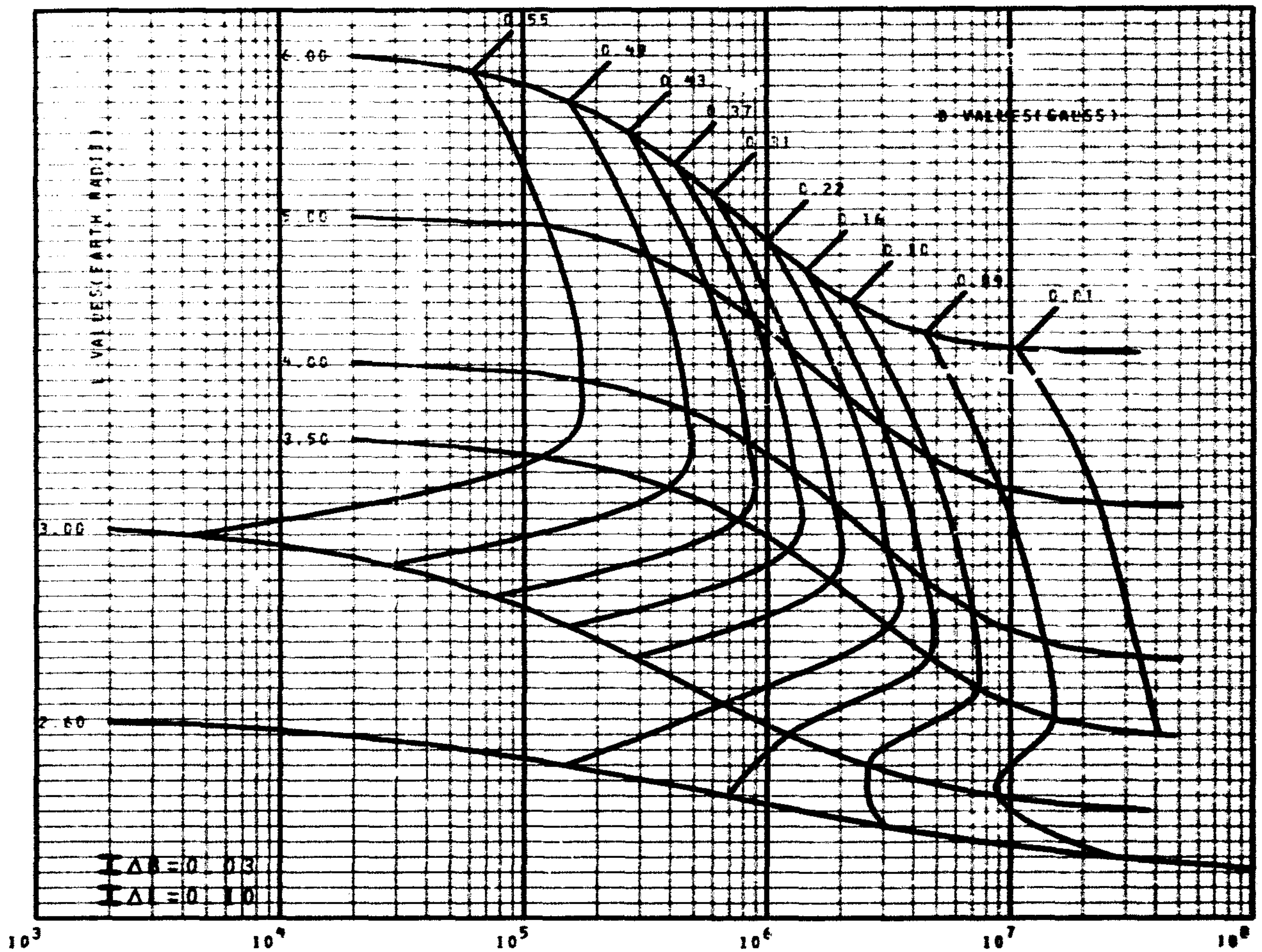

FIGURE 1C OMNIDIRECTIONAL INTEGRAL FLUX MAP

40 KEV ELECTRONS FOR L GE 7.0

MODEL AE4 SOLAR MAXIMUM

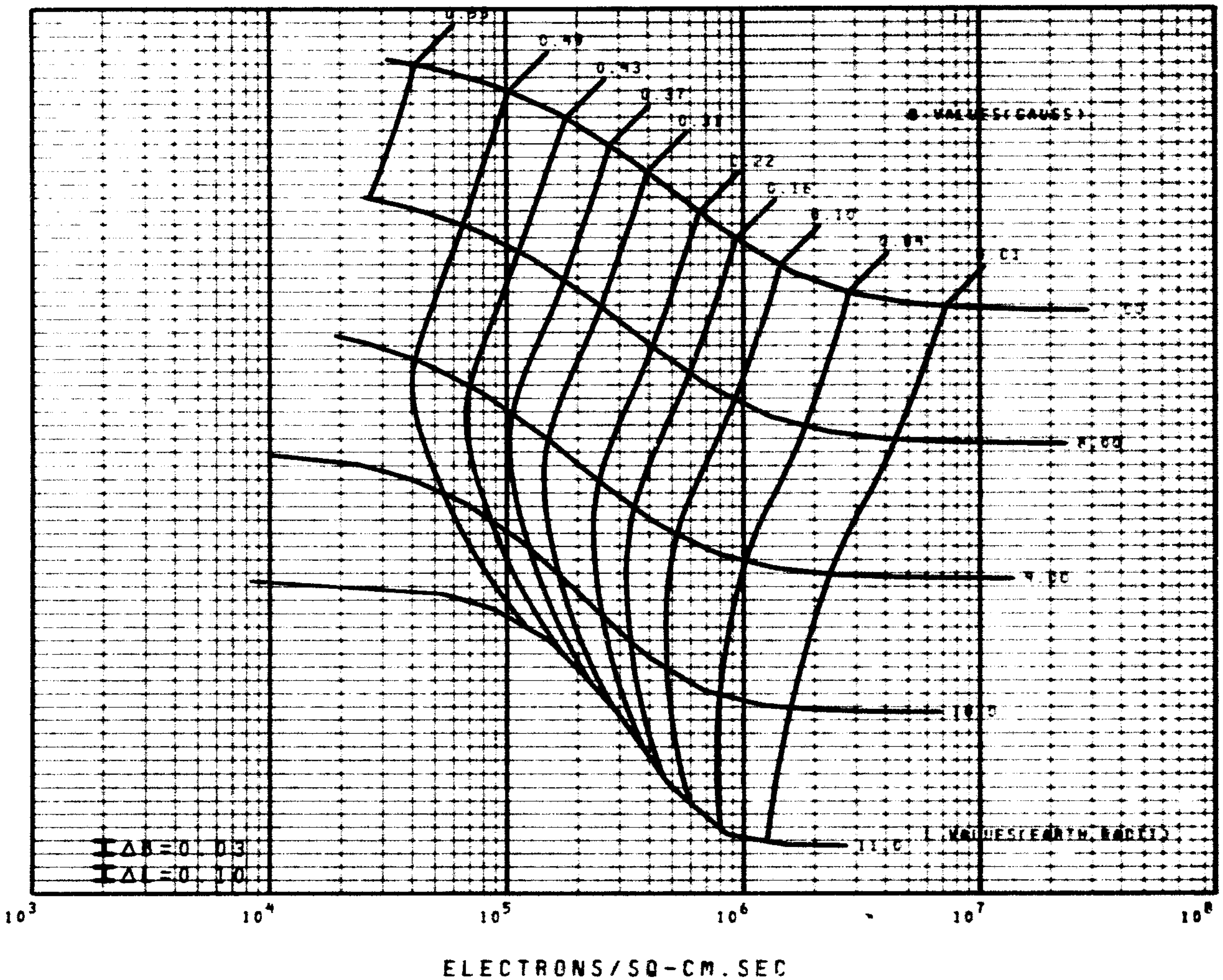

FIGURE 2A OMNIDIRECTIONAL INTEGRAL FLUX MAP

100 KEV ELECTRONS FOR L LE 2.4

MODEL AE6 SOLAR MAXIMUM PROJECTED

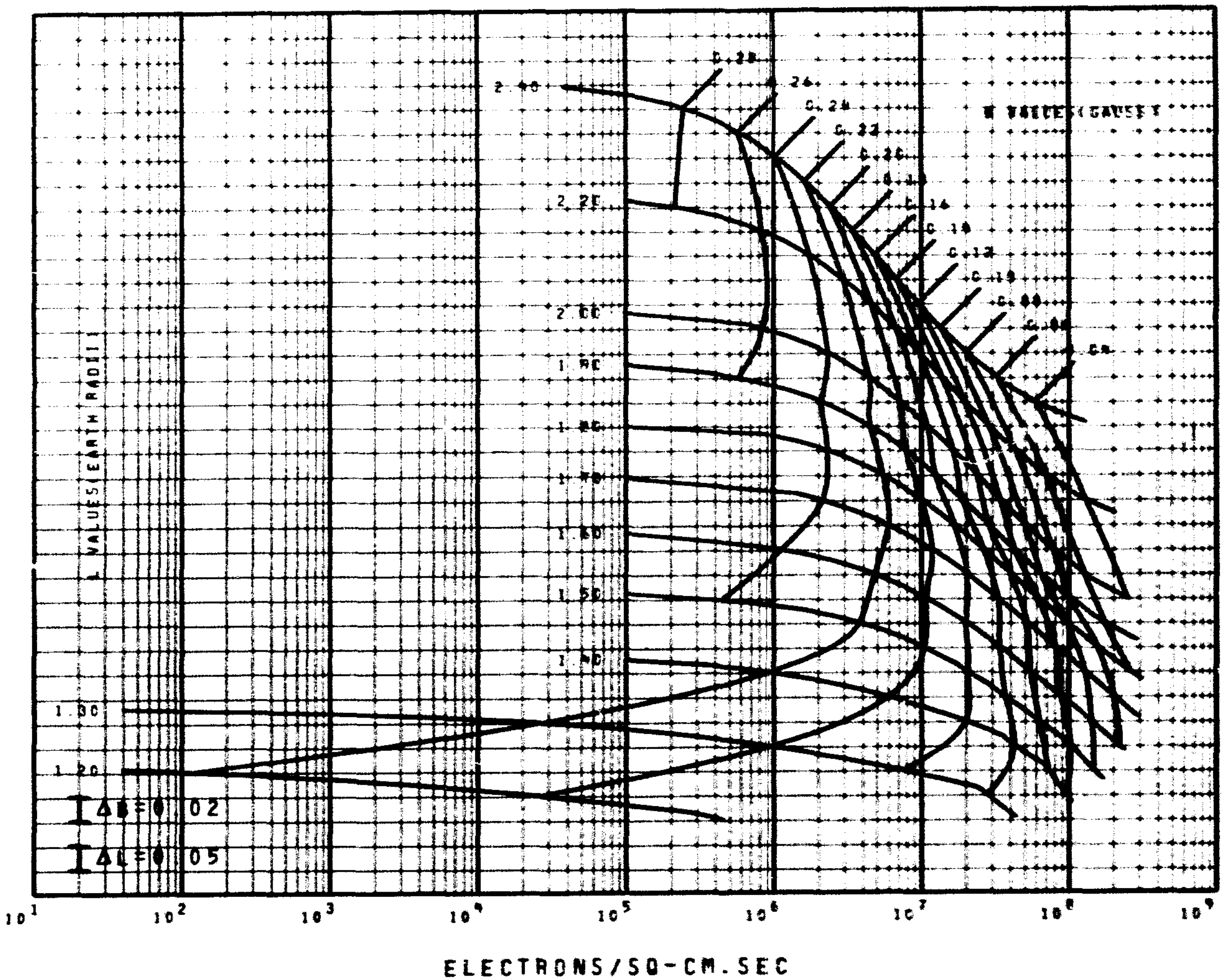

FIGURE 2B OMNIDIRECTIONAL INTEGRAL FLUX MAP

100 KEV ELECTRONS FOR L 2.6 TO 6.0

MODEL AE4 SOLAR MAXIMUM

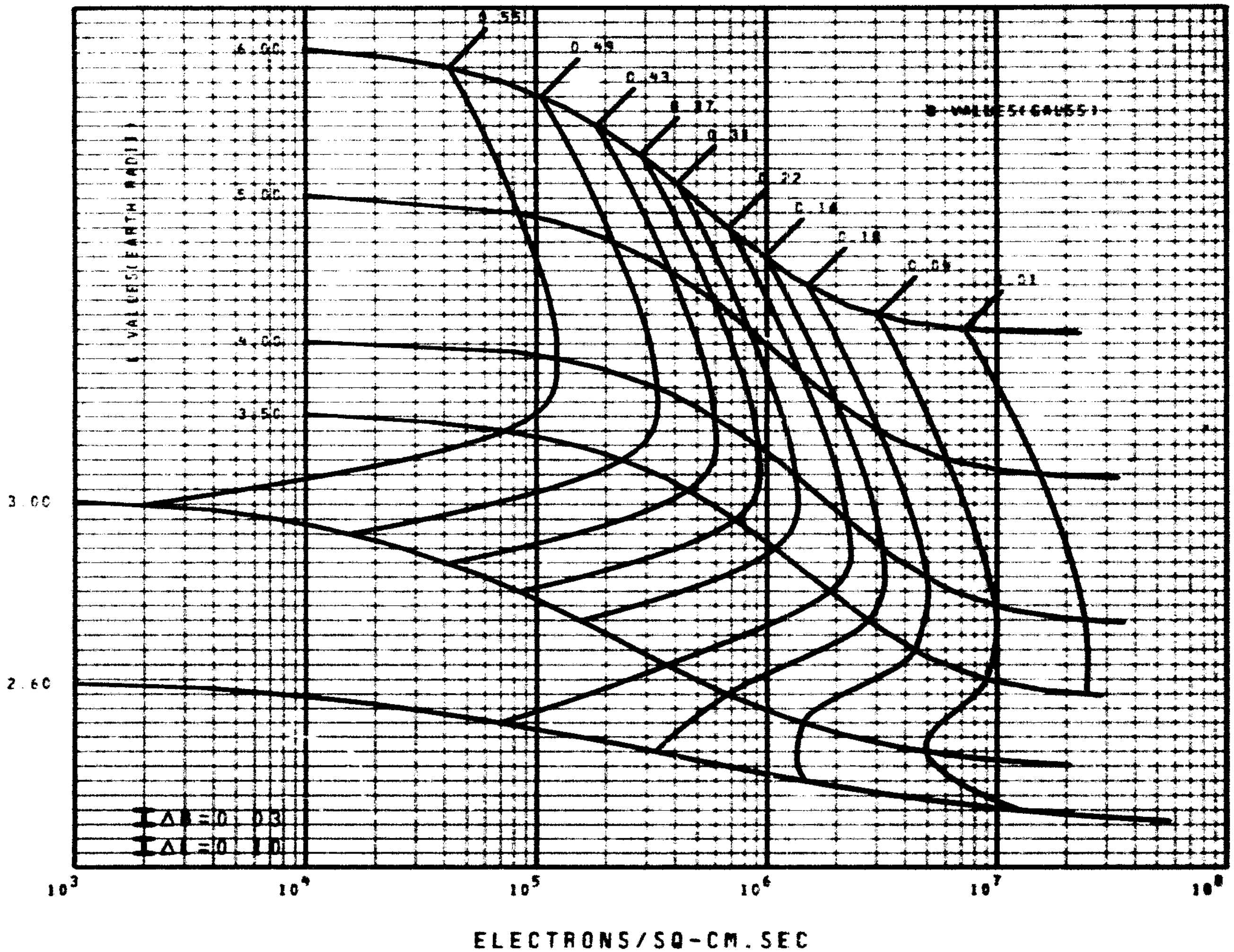

FIGURE 2C OMNIDIRECTIONAL INTEGRAL FLUX MAP

100 KEV ELECTRONS FOR L GE 7.0

MODEL AE4 SOLAR MAXIMUM

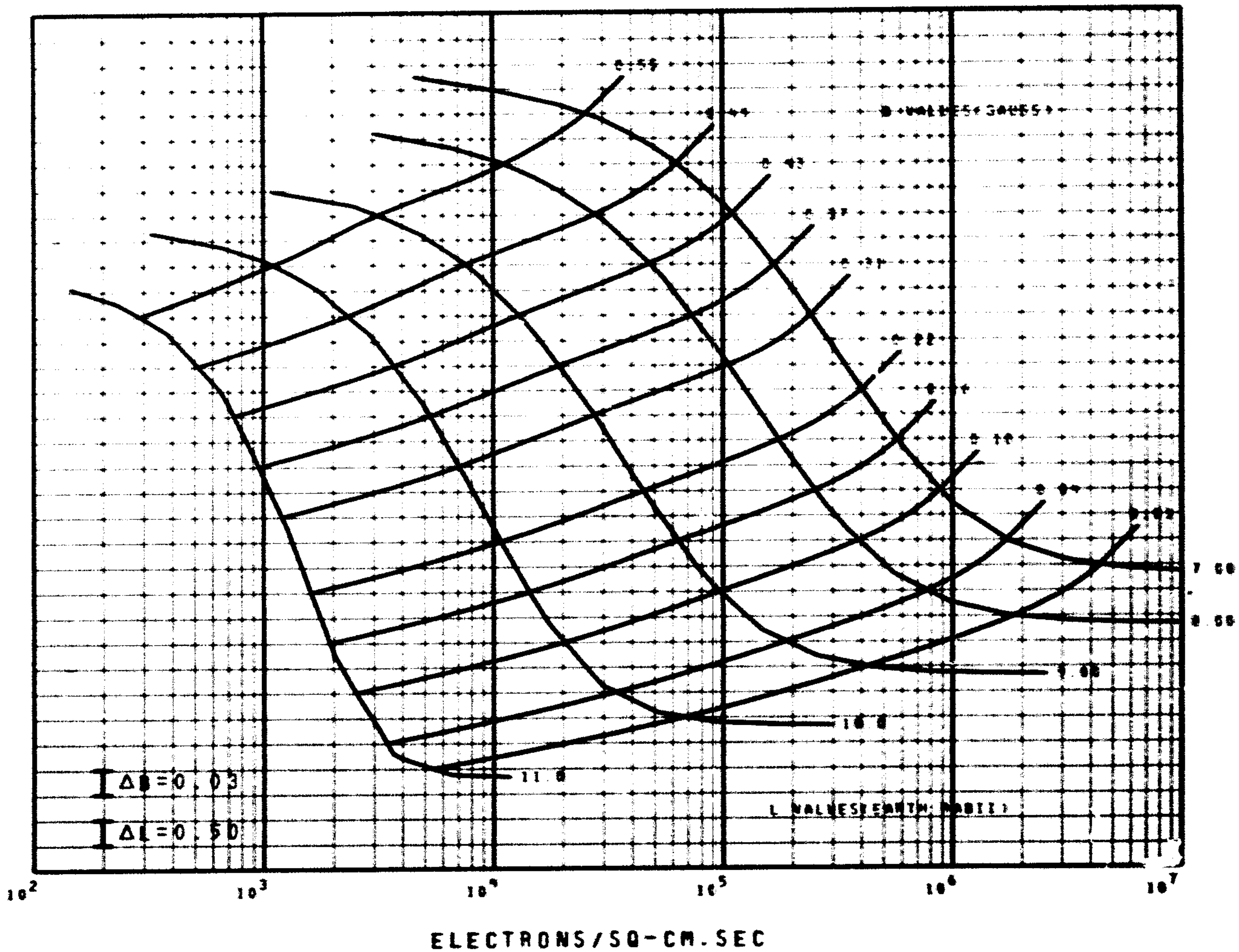

FIGURE 3A OMNIDIRECTIONAL INTEGRAL FLUX MAP

250 KEV ELECTRONS FOR L LE 2.4

MODEL AE6 SOLAR MAXIMUM PROJECTED

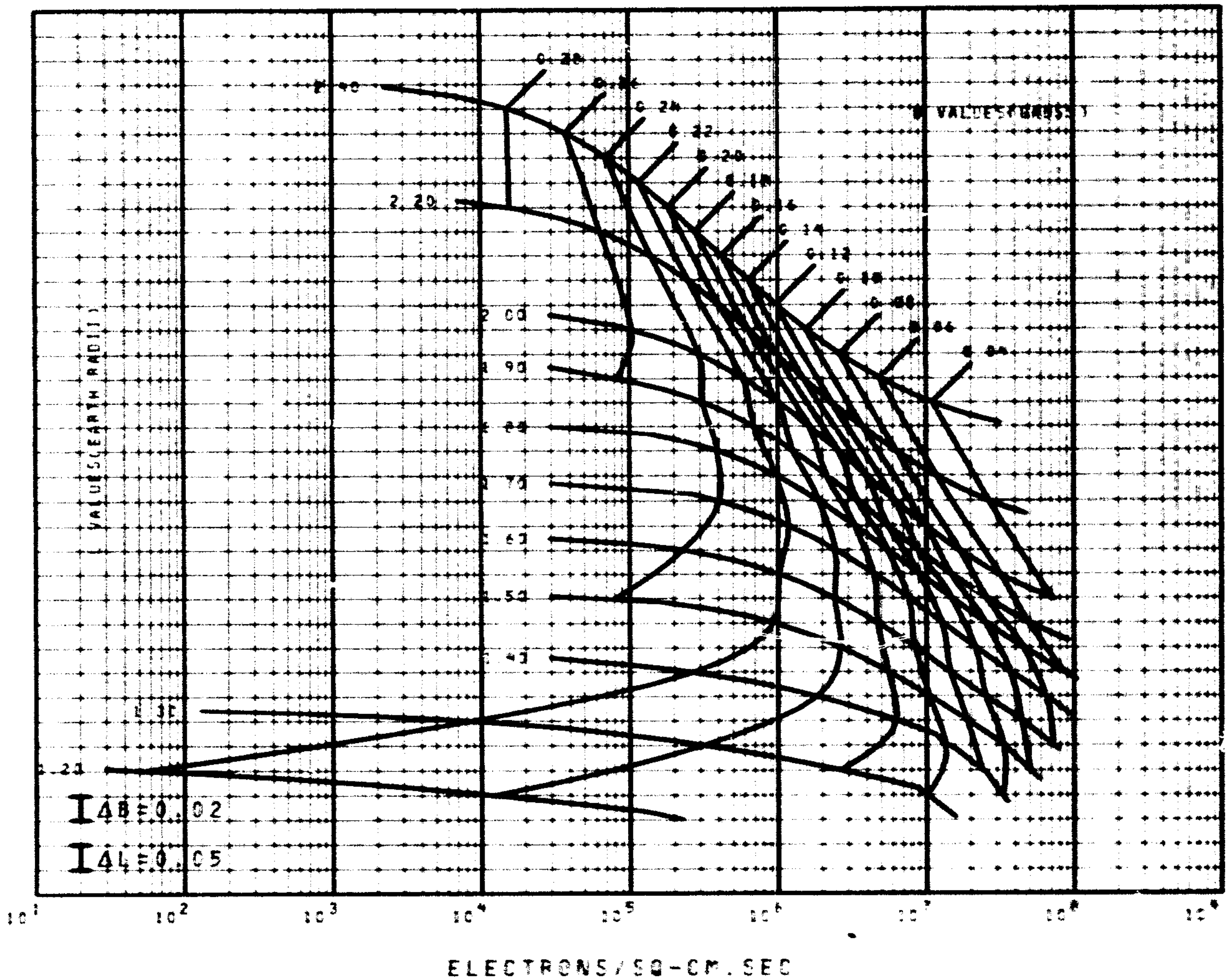

FIGURE 3B OMNIDIRECTIONAL INTEGRAL FLUX MAP

250 KEV ELECTRONS FOR L 2.6 TO 5.0

MODEL AE4 SOLAR MAXIMUM

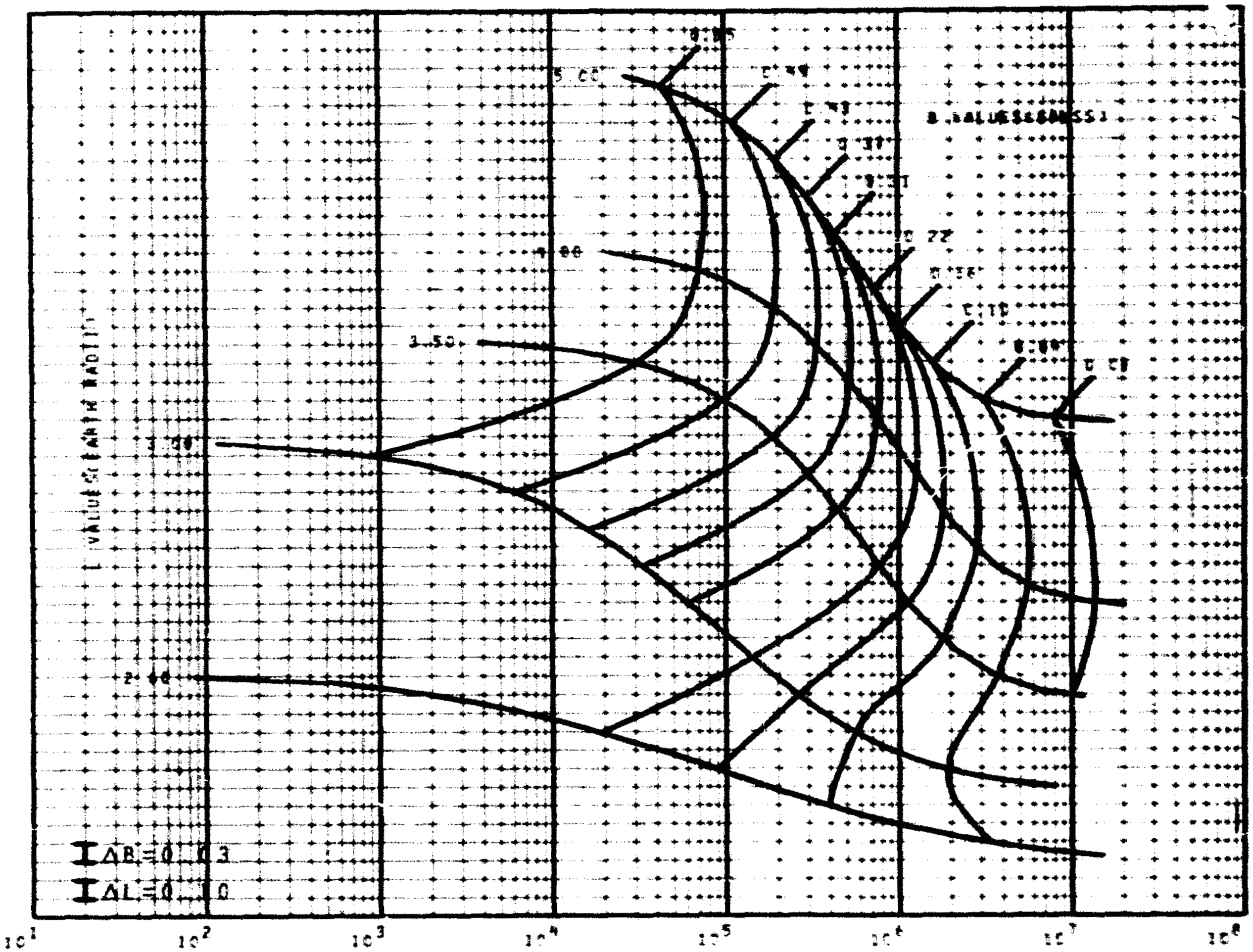

FIGURE 3C OMNIDIRECTIONAL INTEGRAL FLUX MAP

250 KEV ELECTRONS FOR L GE 6.0

MODEL AE4 SOLAR MAXIMUM

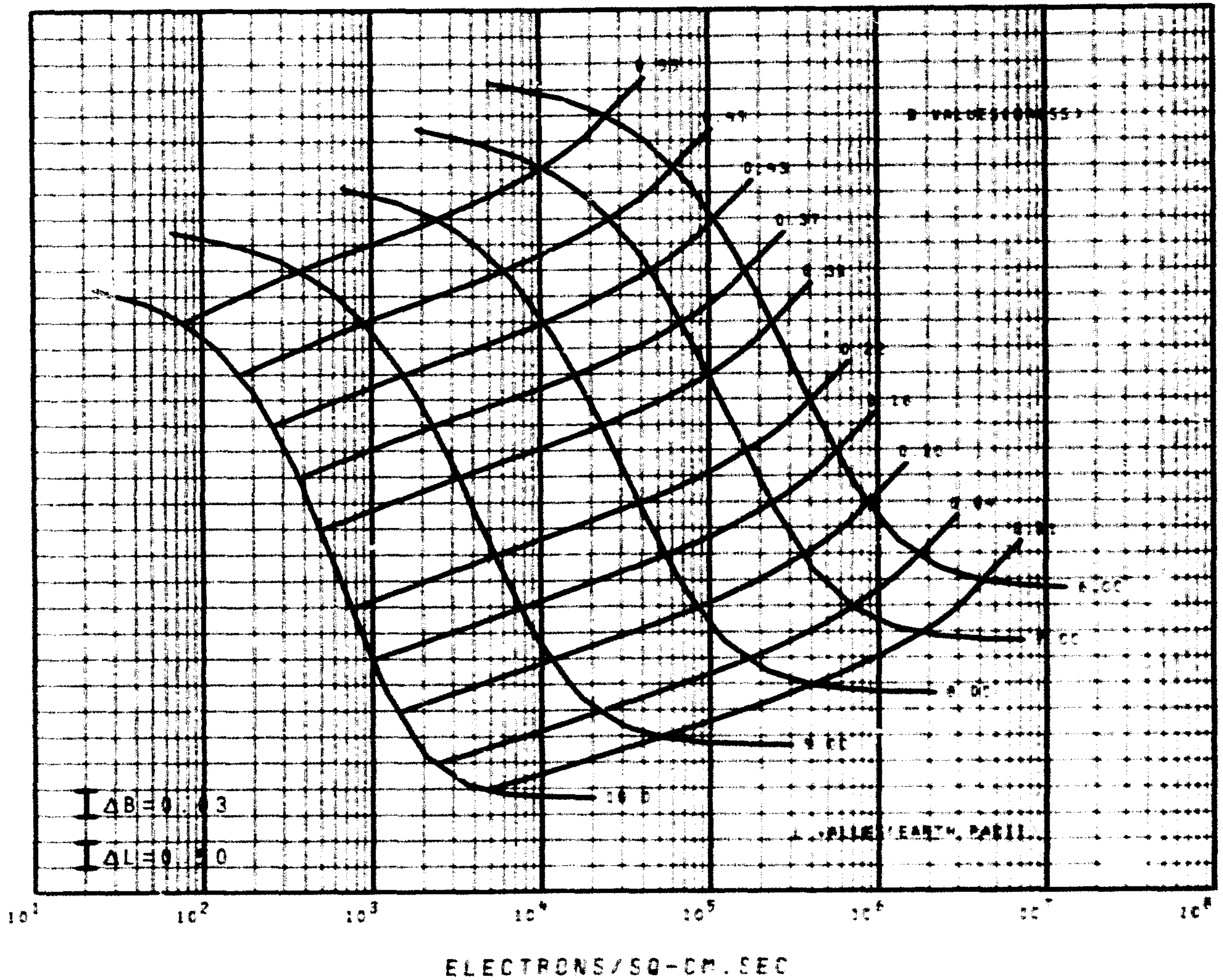

FIGURE 4A OMNIDIRECTIONAL INTEGRAL FLUX MAP

500 KEV ELECTRONS FOR L LE 2.4

MODEL AE6 SOLAR MAXIMUM PROJECTED

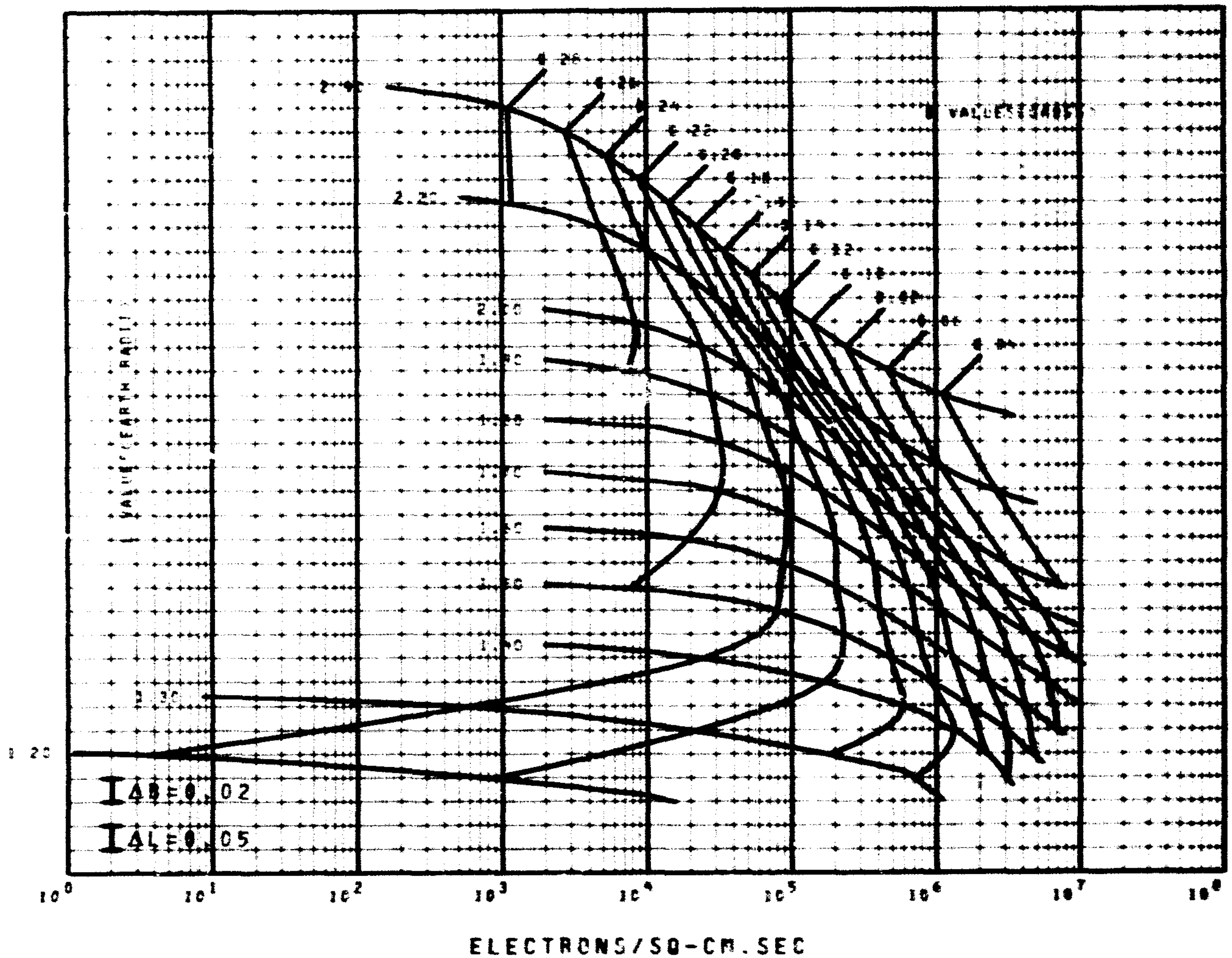

22

FIGURE 4B OMNIDIRECTIONAL INTEGRAL FLUX MAP

500 KEV ELECTRONS FOR L 2.6 TO 5.0

MODEL AE4 SOLAR MAXIMUM

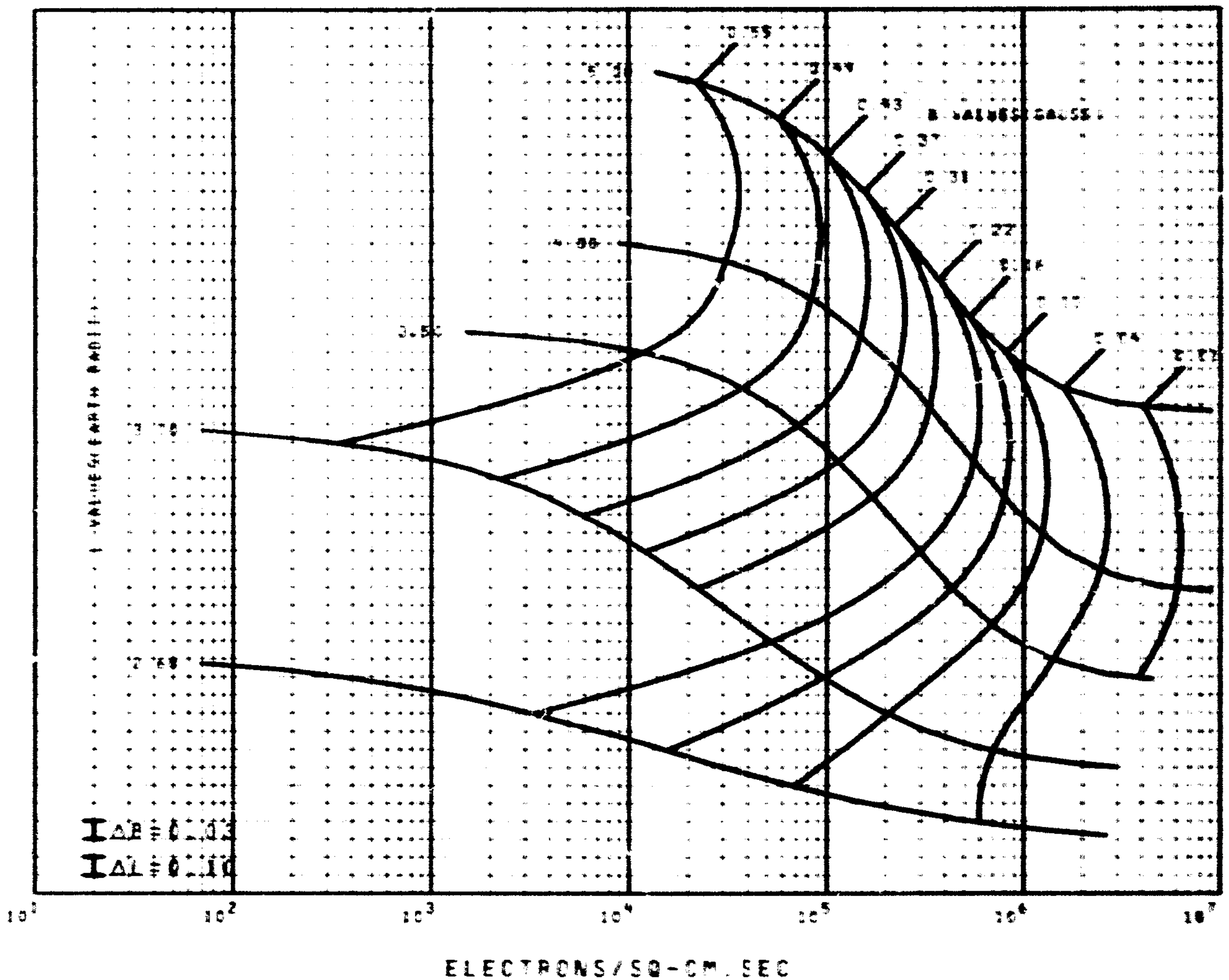

FIGURE 4C OMNIDIRECTIONAL INTEGRAL FLUX MAP

500 KEV ELECTRONS FOR L GE 6.0

MODEL AE4 SOLAR MAXIMUM

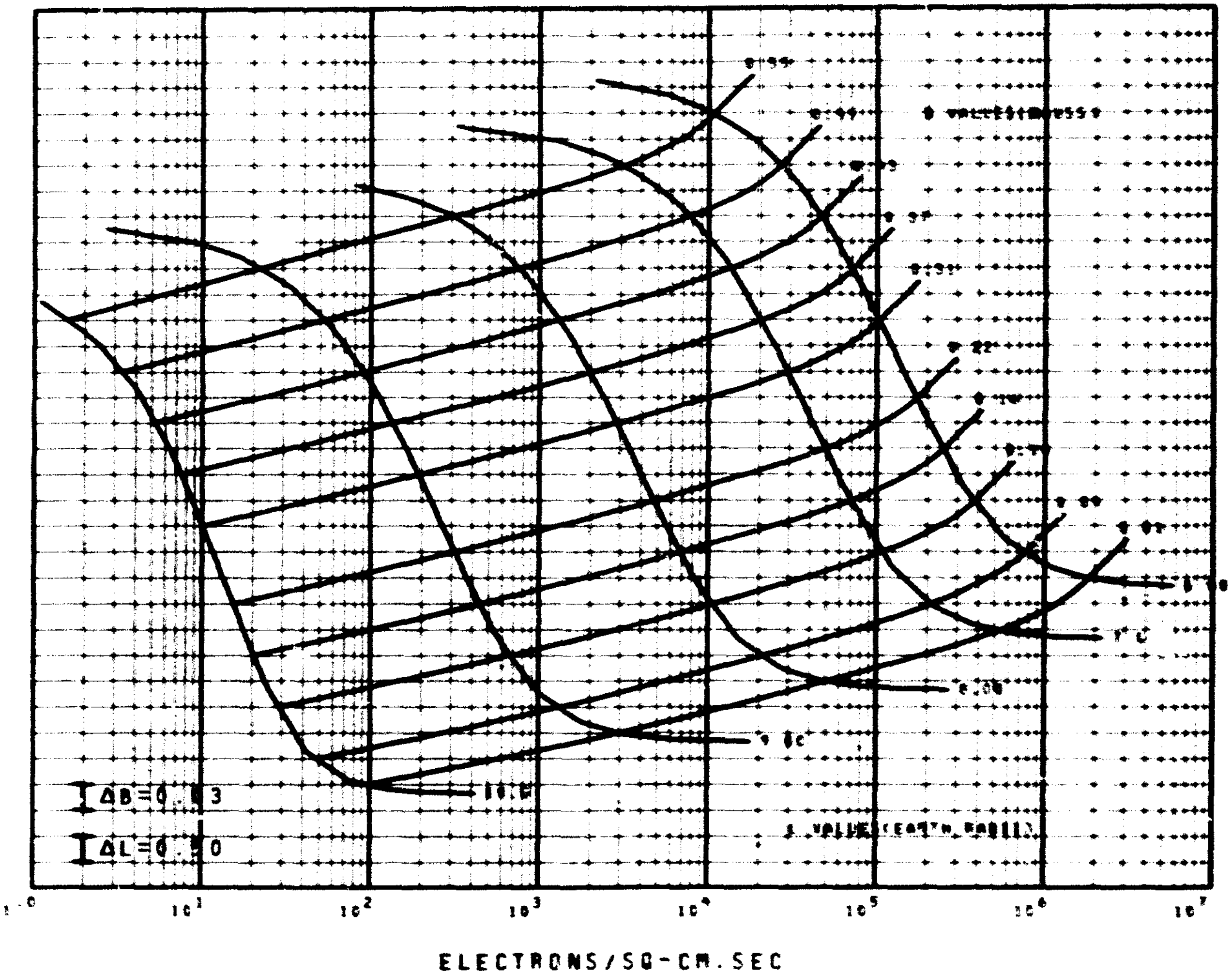

FIGURE 5A OMNIDIRECTIONAL INTEGRAL FLUX MAP

750 KEV ELECTRONS FOR L LE 2.4

MODEL AE6 SOLAR MAXIMUM PROJECTED

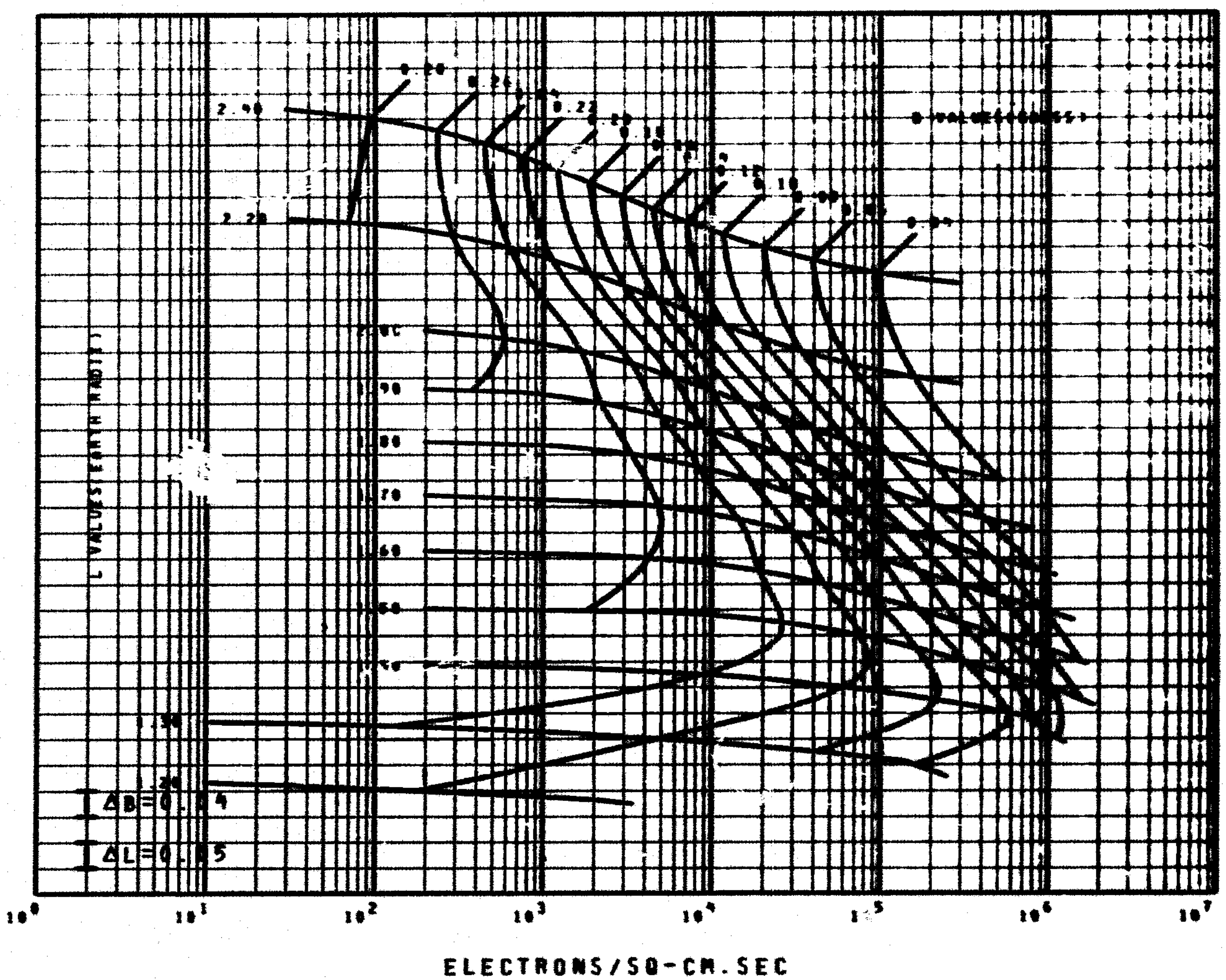

FIGURE 5B OMNIDIRECTIONAL INTEGRAL FLUX MAP

750 KEV ELECTRONS FOR L 2.6 TO 5.0

MODEL AE4 SOLAR MAXIMUM

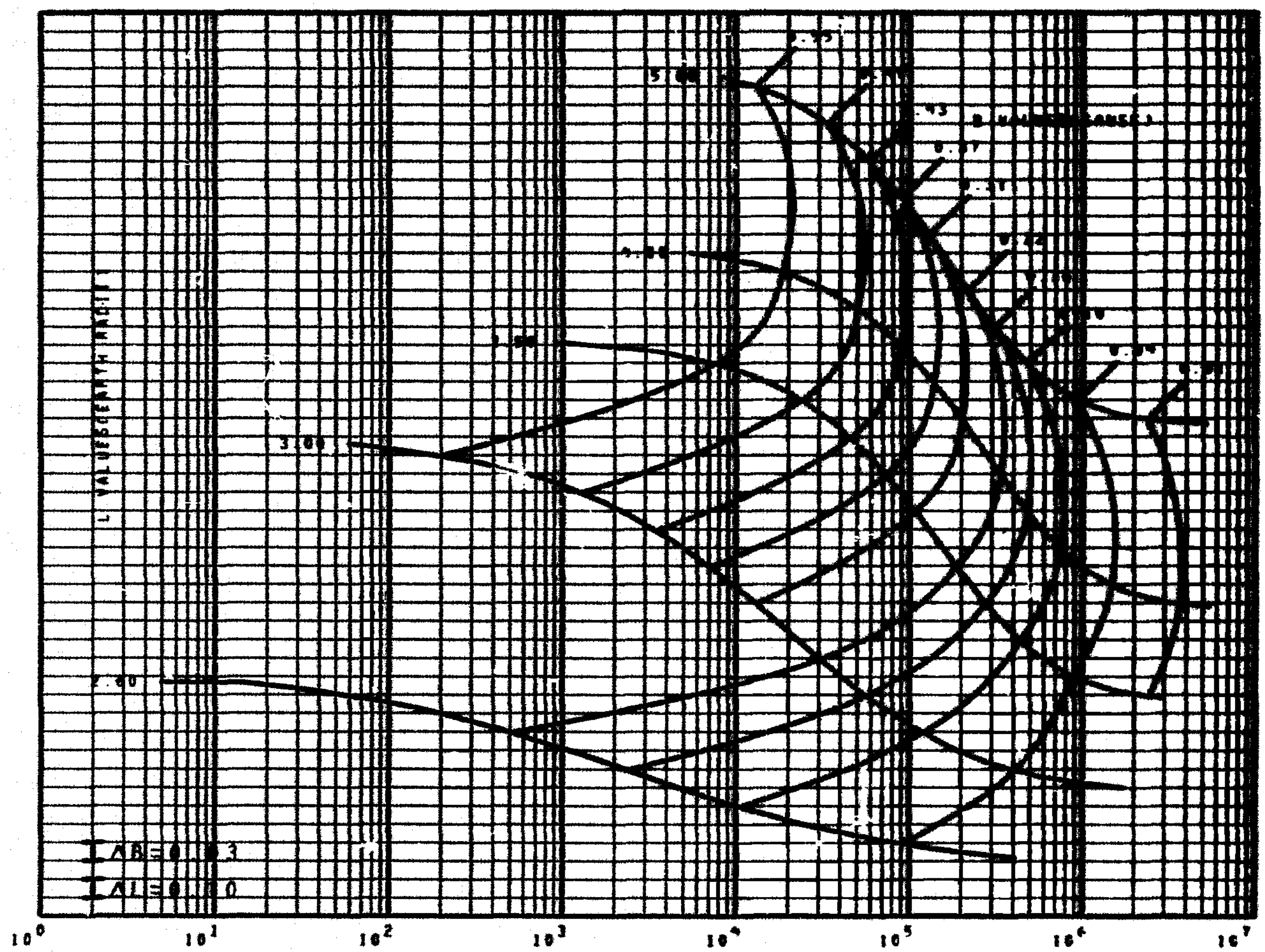

ELECTRONS/SQ-CM.SEC

FIGURE 5C OMNIDIRECTIONAL INTEGRAL FLUX MAP

750 KEV ELECTRONS FOR L CE 6.0

MODEL AE4 SOLAR MAXIMUM

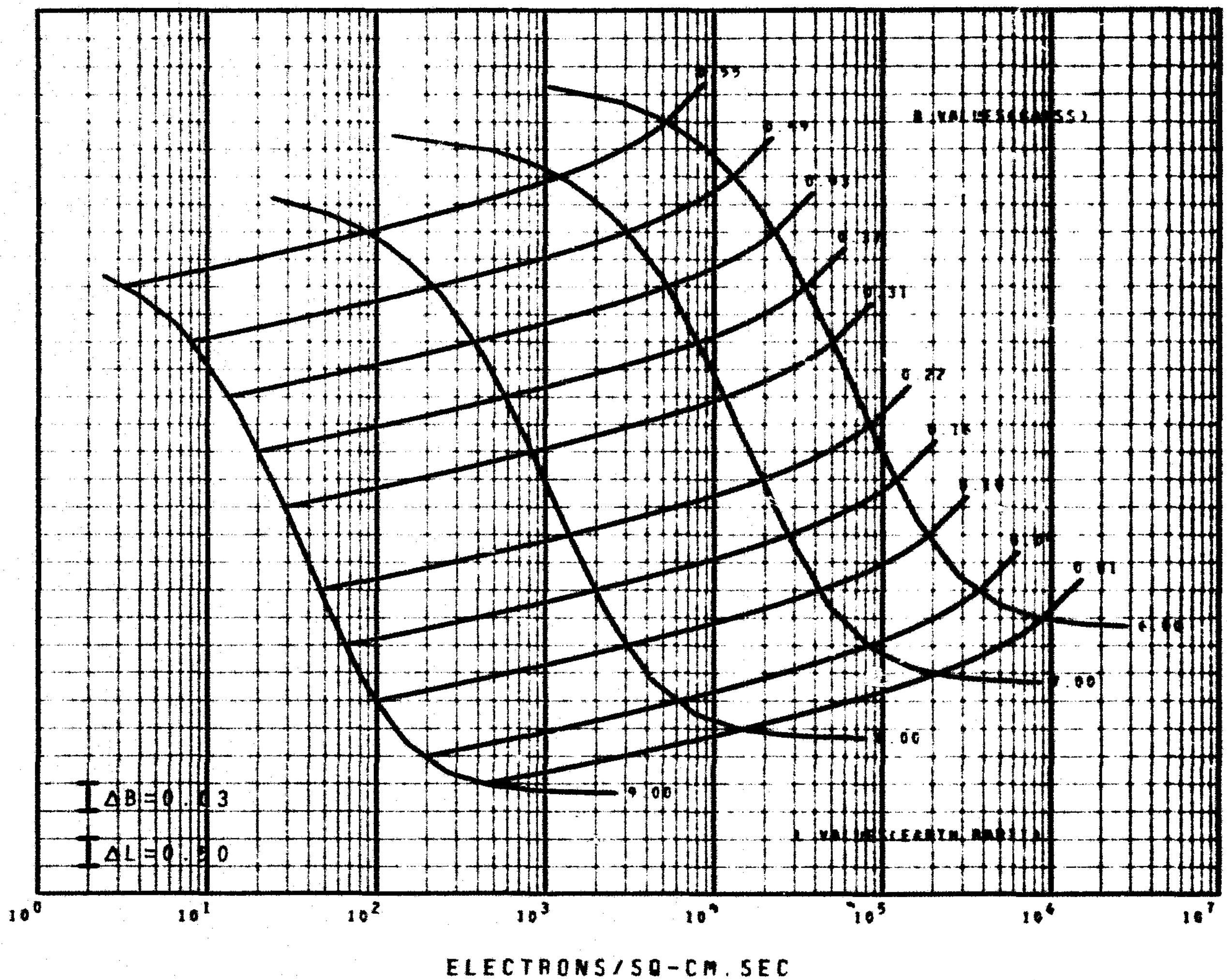

FIGURE 6A OMNIDIRECTIONAL INTEGRAL FLUX MAP

1.0 MEV ELECTRONS FOR L LE 2.4

MODEL AE6 SOLAR MAXIMUM PROJECTED

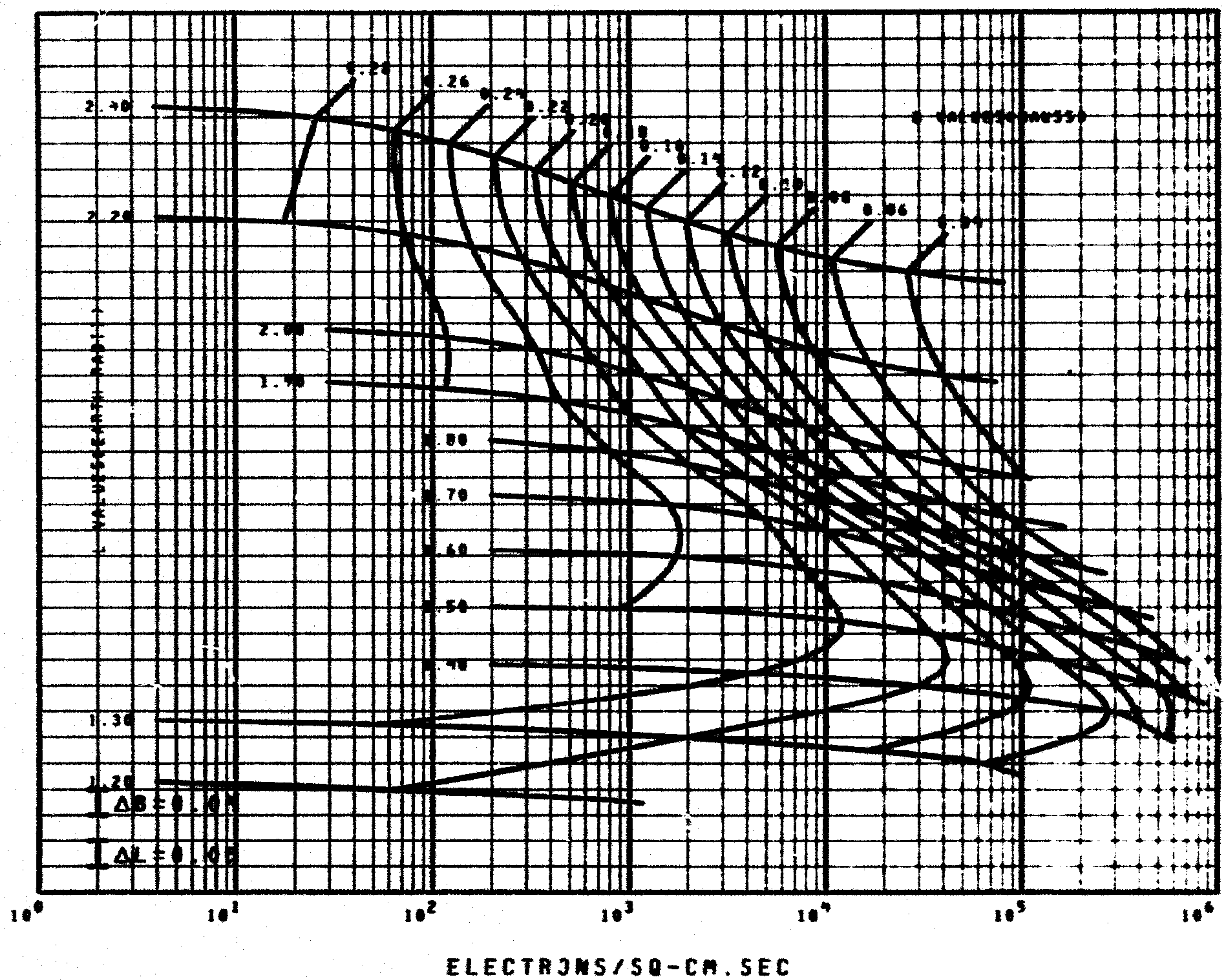

FIGURE 6B OMNIDIRECTIONAL INTEGRAL FLUX MAP

1.0 MEV ELECTRONS FOR L 2.6 TO 5.0

MODEL AE4 SOLAR MAXIMUM

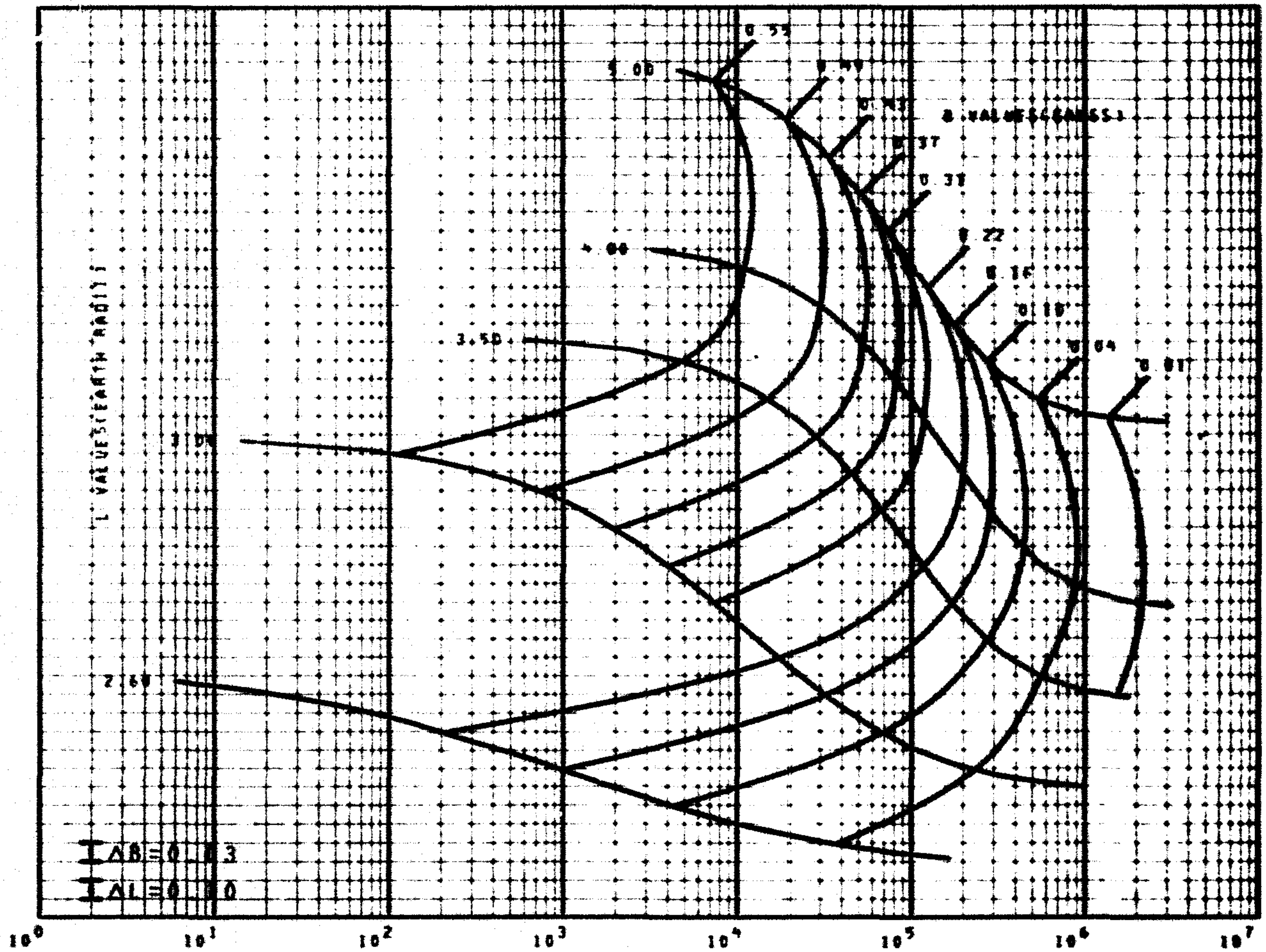

FIGURE 6C OMNIDIRECTIONAL INTEGRAL FLUX MAP

1.0 MEV ELECTRONS FOR L GE 6.0

MODEL AE4 SOLAR MAXIMUM

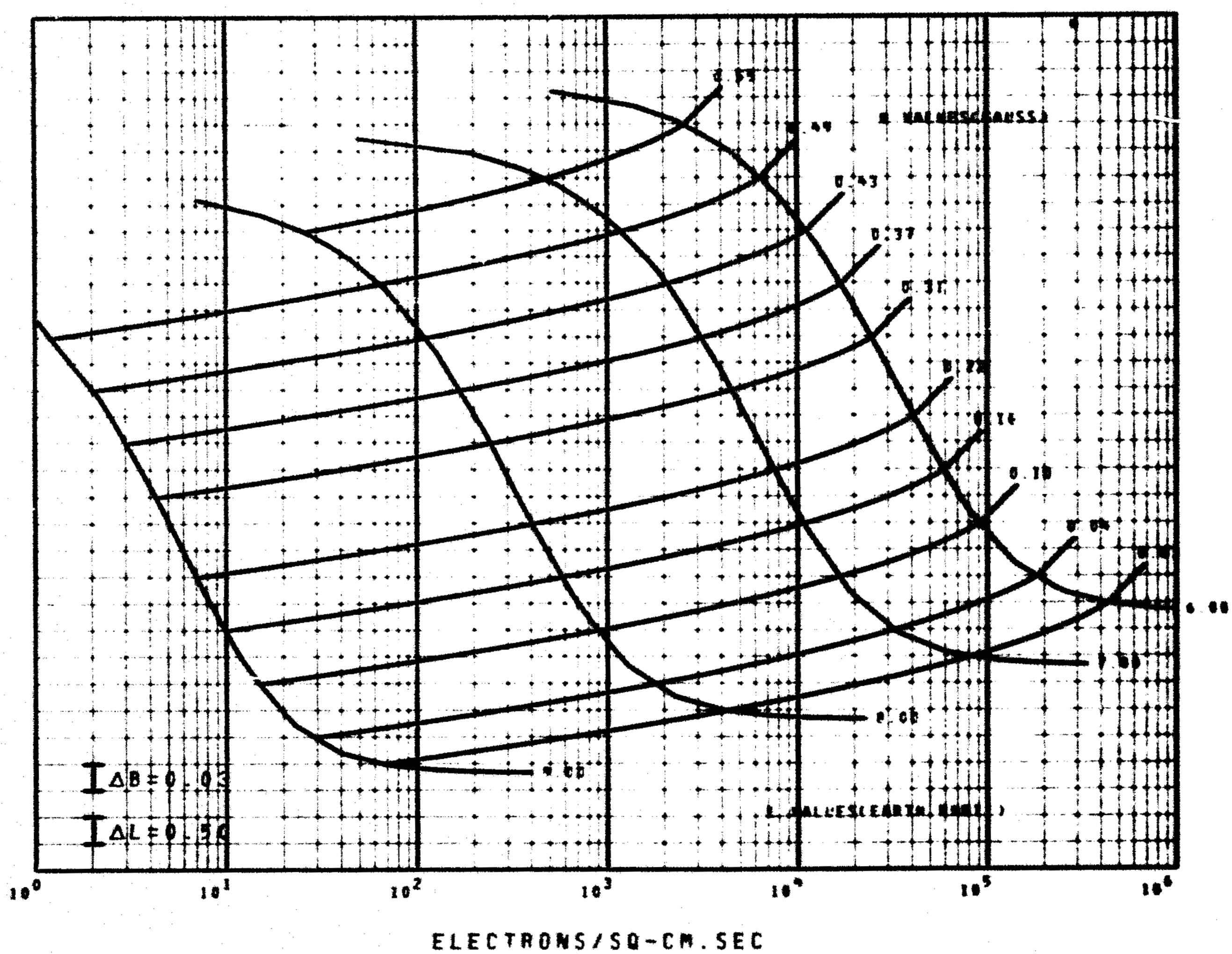

FIGURE 7A OMNIDIRECTIONAL INTEGRAL FLUX MAP

2.0 MEV ELECTRONS FOR L LE 2.4

MODEL AE6 SOLAR MAXIMUM PROJECTED

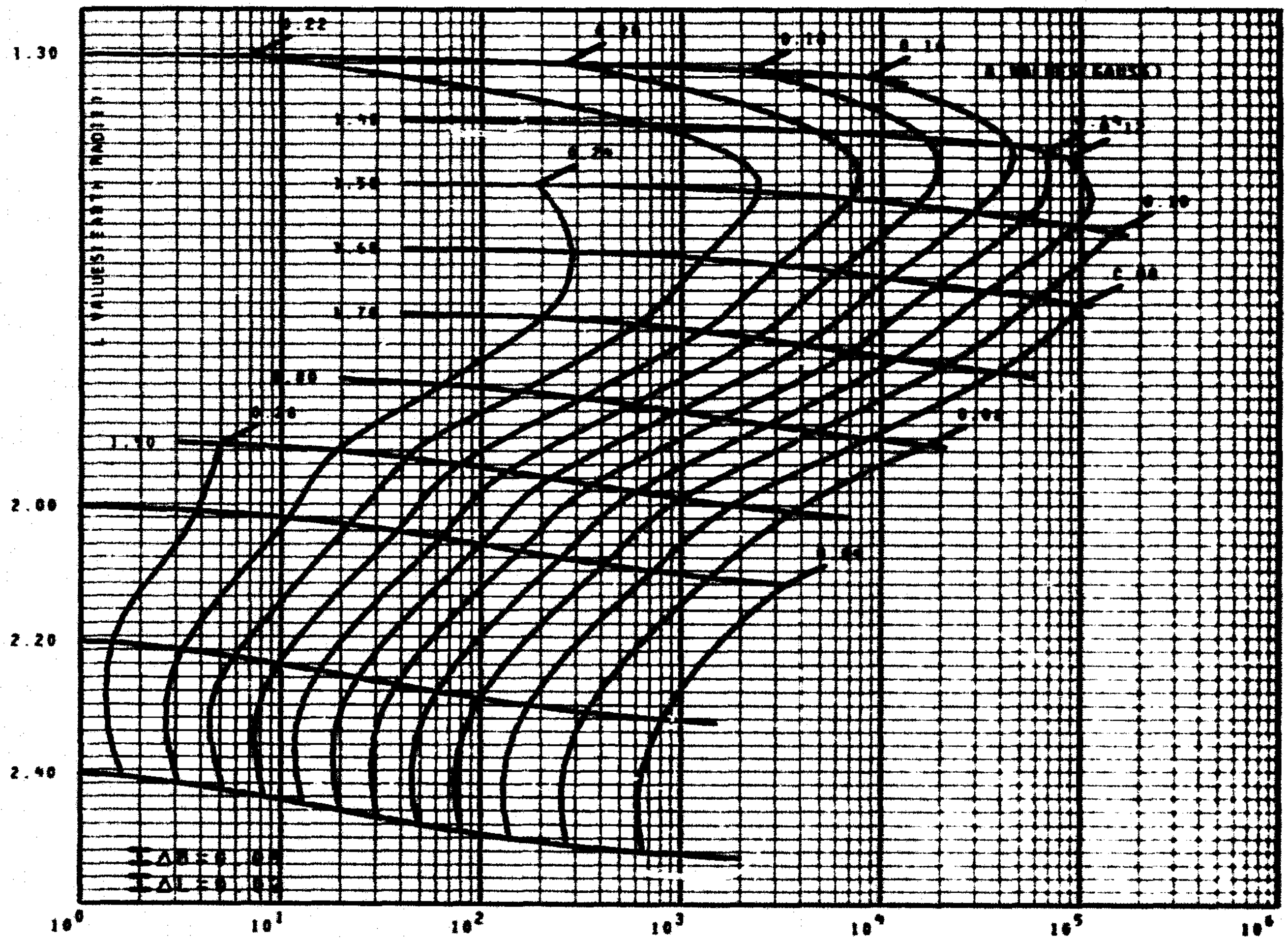

FIGURE 7B OMNIDIRECTIONAL INTEGRAL FLUX MAP
2.0 MEV ELECTRONS FOR L 2.6 TO 4.0
MODEL AE4 SOLAR MAXIMUM

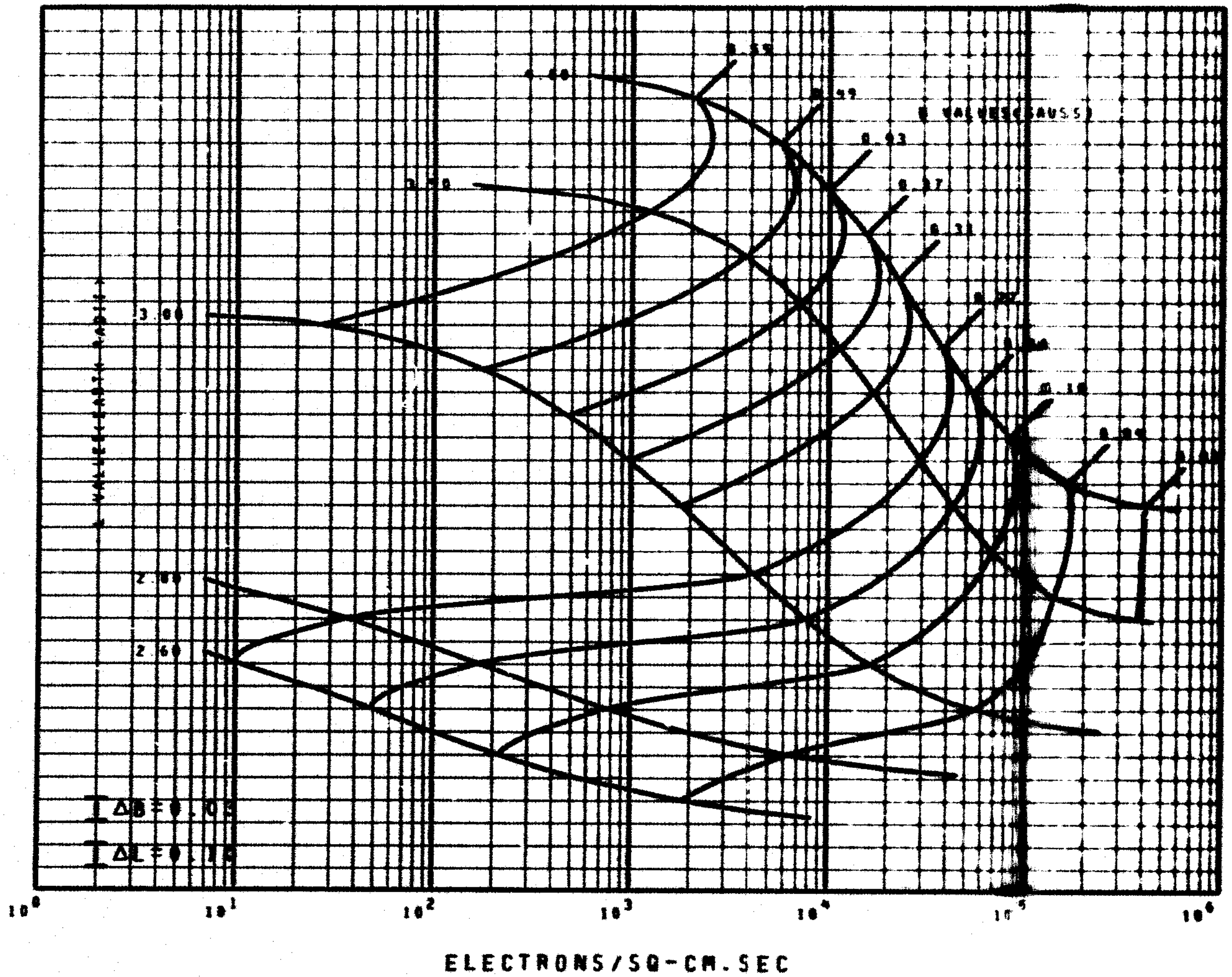

FIGURE 7C OMNIDIRECTIONAL INTEGRAL FLUX MAP

2.0 MEV ELECTRONS FOR L GE 5.0

MODEL AE4 SOLAR MAXIMUM

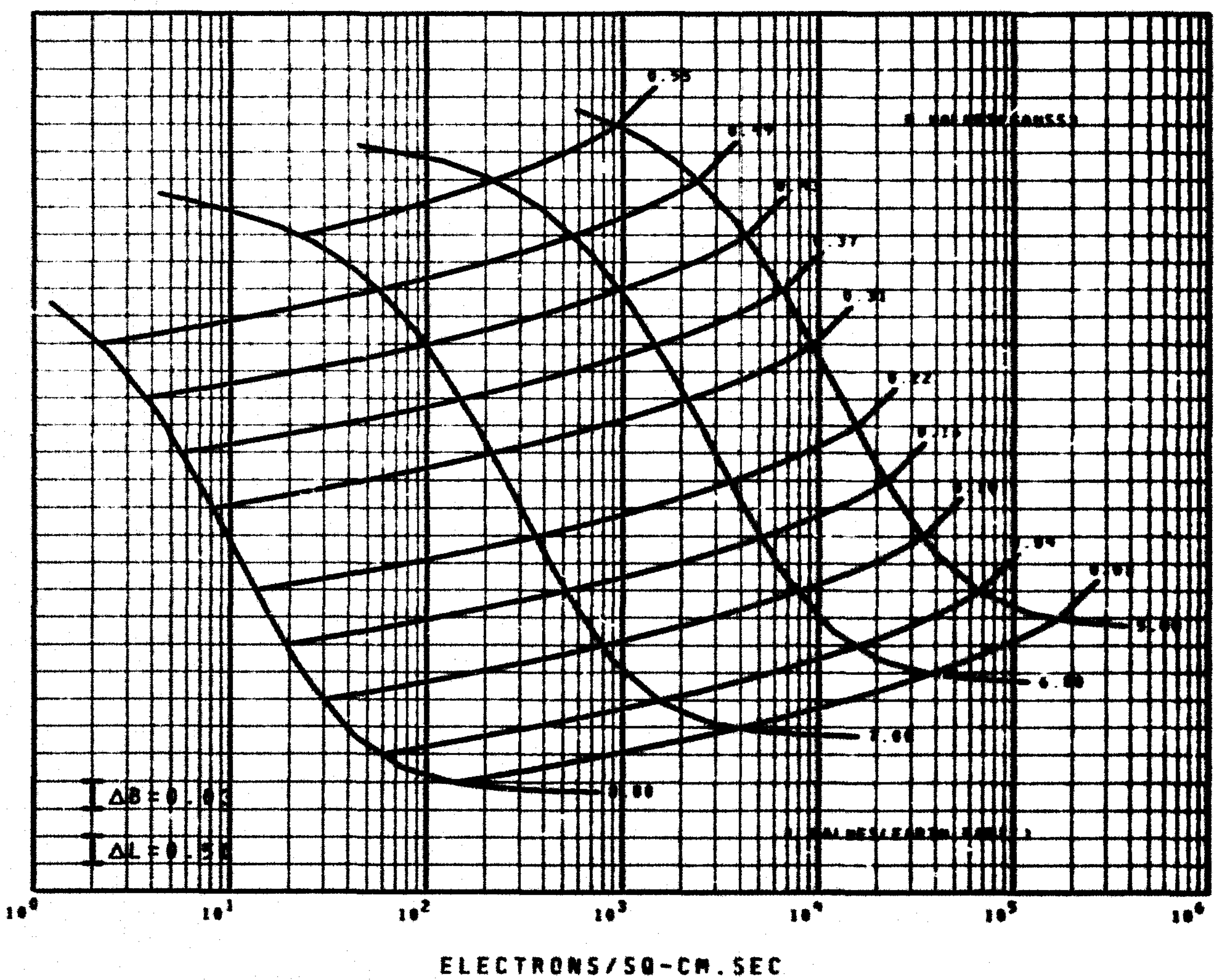

FIGURE 8A OMNIDIRECTIONAL INTEGRAL FLUX MAP

3.0 MEV ELECTRONS FOR L LE 2.4

MODEL AE6 SOLAR MAXIMUM PROJECTED

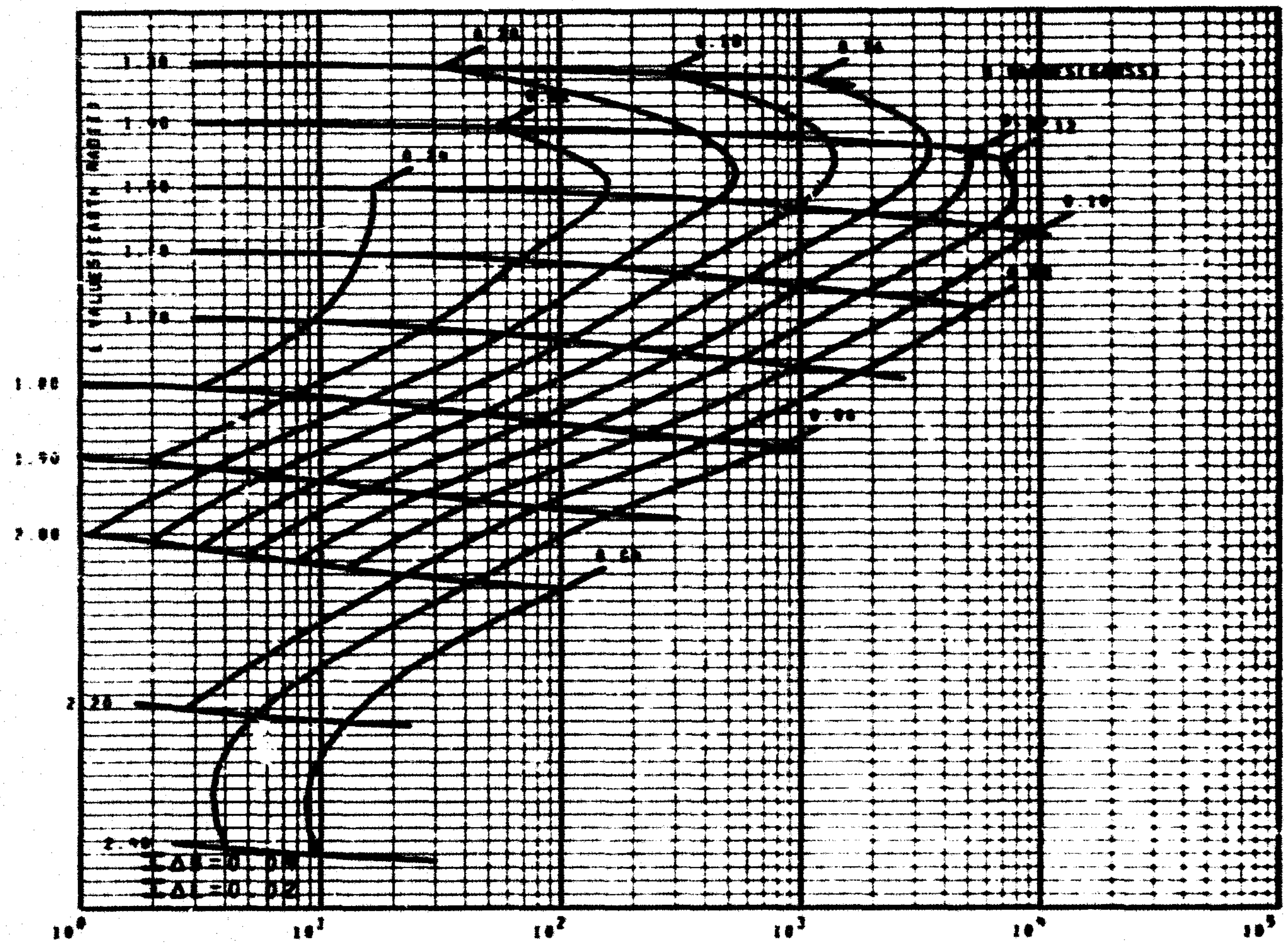

ELECTRONS/SQ-CM.SEC

FIGURE 8B OMNIDIRECTIONAL INTEGRAL FLUX MAP

3.0 MEV ELECTRONS FOR L 2.6 TO 4.0

MODEL AE4 SOLAR MAXIMUM

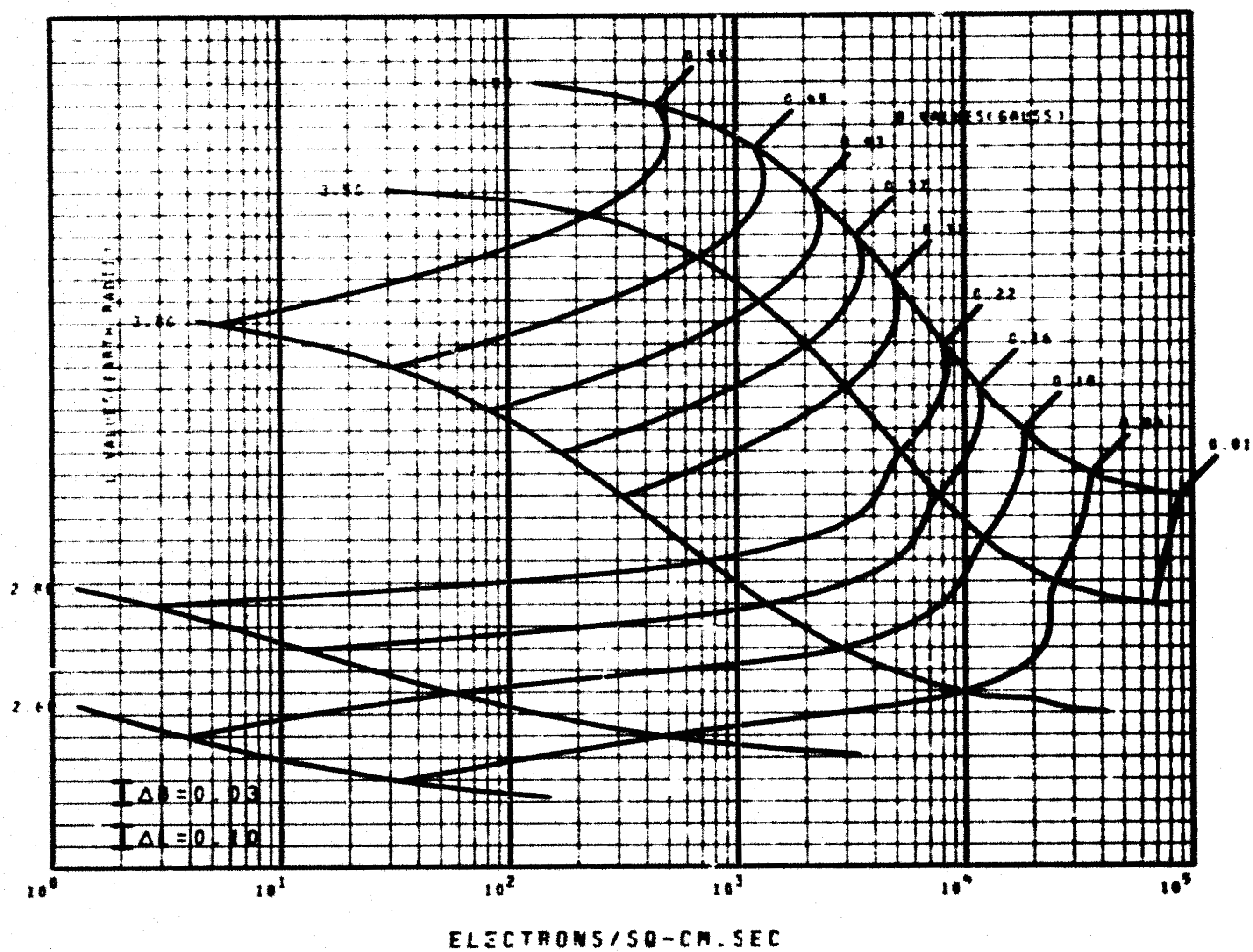

FIGURE 8C OMNIDIRECTIONAL INTEGRAL FLUX MAP

3.0 MEV ELECTRONS FOR L GE 5.0

MODEL AE4 SOLAR MAXIMUM

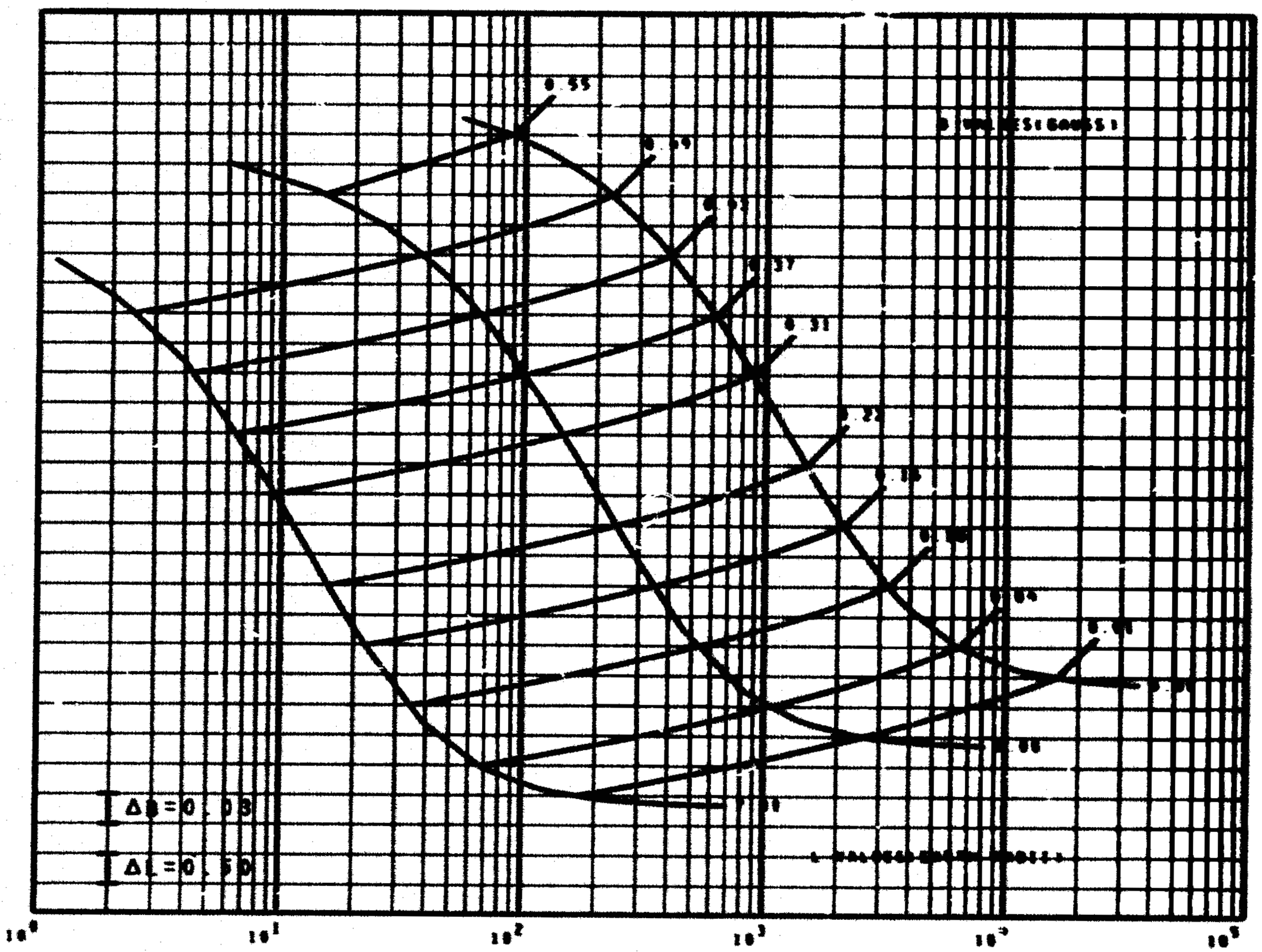

ELECTRONS/SQ-CM.SEC

FIGURE 9A OMNIDIRECTIONAL INTEGRAL FLUX MAP

4.0 MEV ELECTRONS FOR L LE 2.4

MODEL AE6 SOLAR MAXIMUM PROJECTED

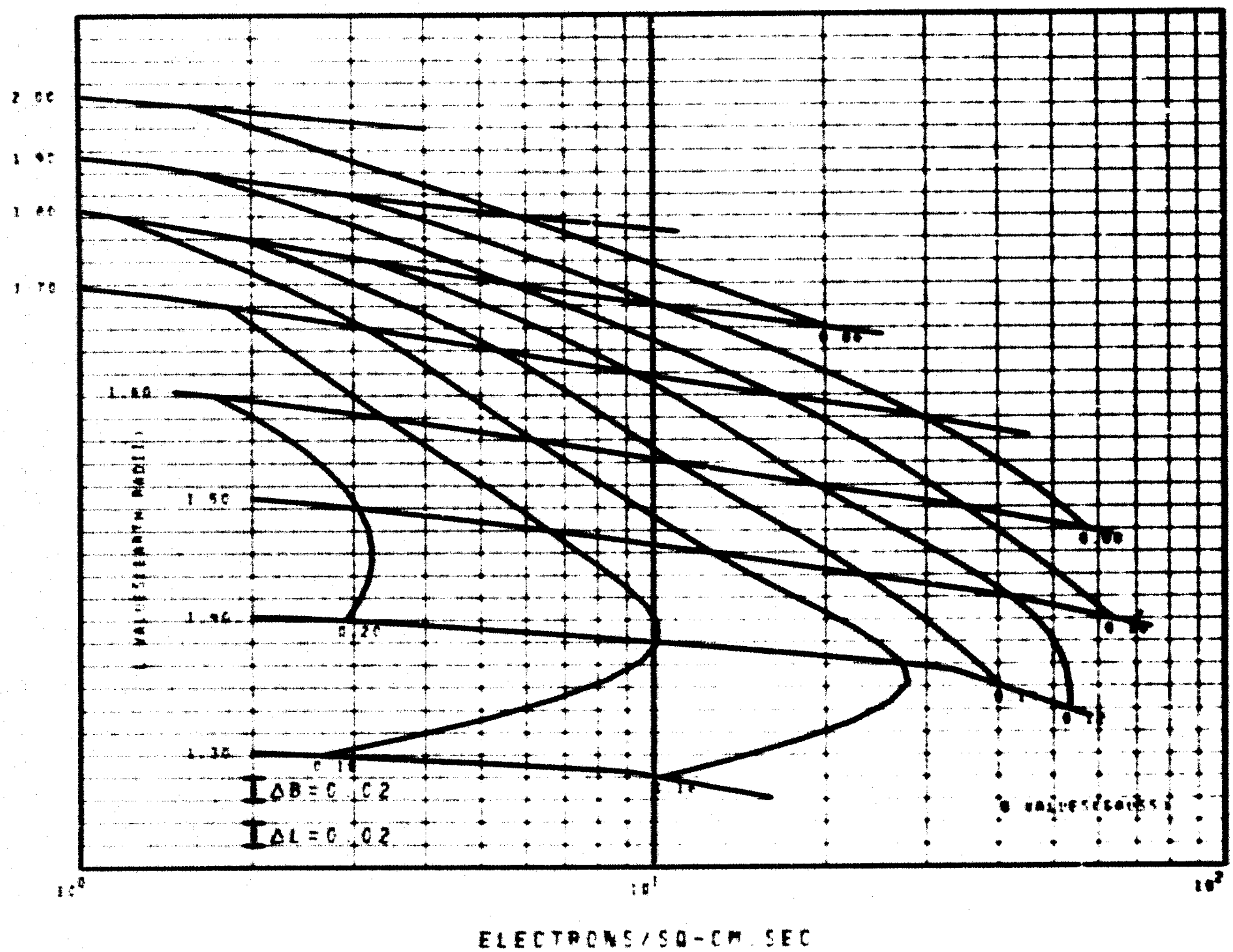

FIGURE 9B OMNIDIRECTIONAL INTEGRAL FLUX MAP

4.0 MEV ELECTRONS FOR L 2.0 TO 4.0

MODEL AE4 SOLAR MAXIMUM

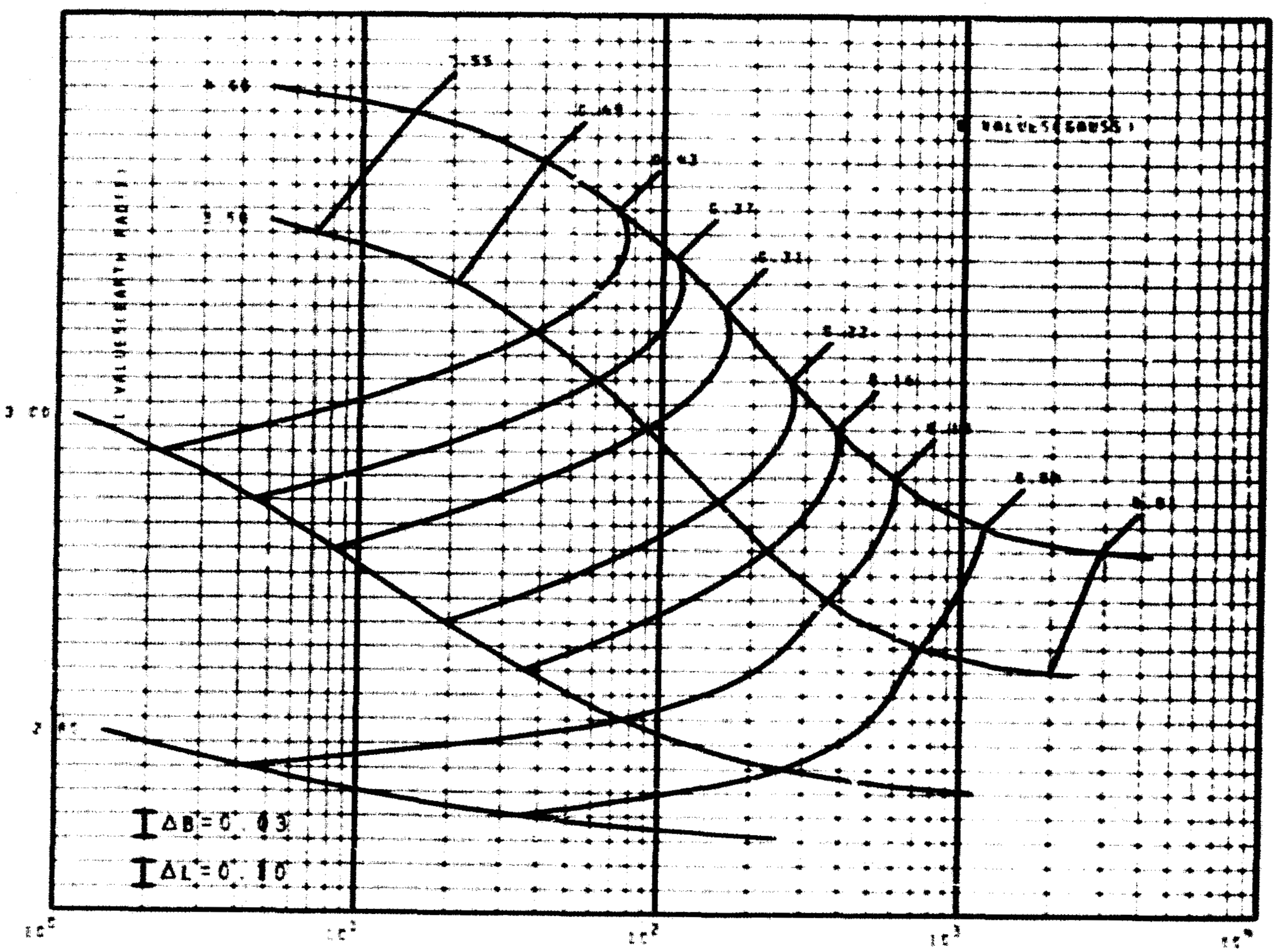

ELECTRONS/SQ-CM SEC

FIGURE 9C OMNIDIRECTIONAL INTEGRAL FLUX MAP

4.0 MEV ELECTRONS FOR L GE 4.5

MODEL AE4 SOLAR MAXIMUM

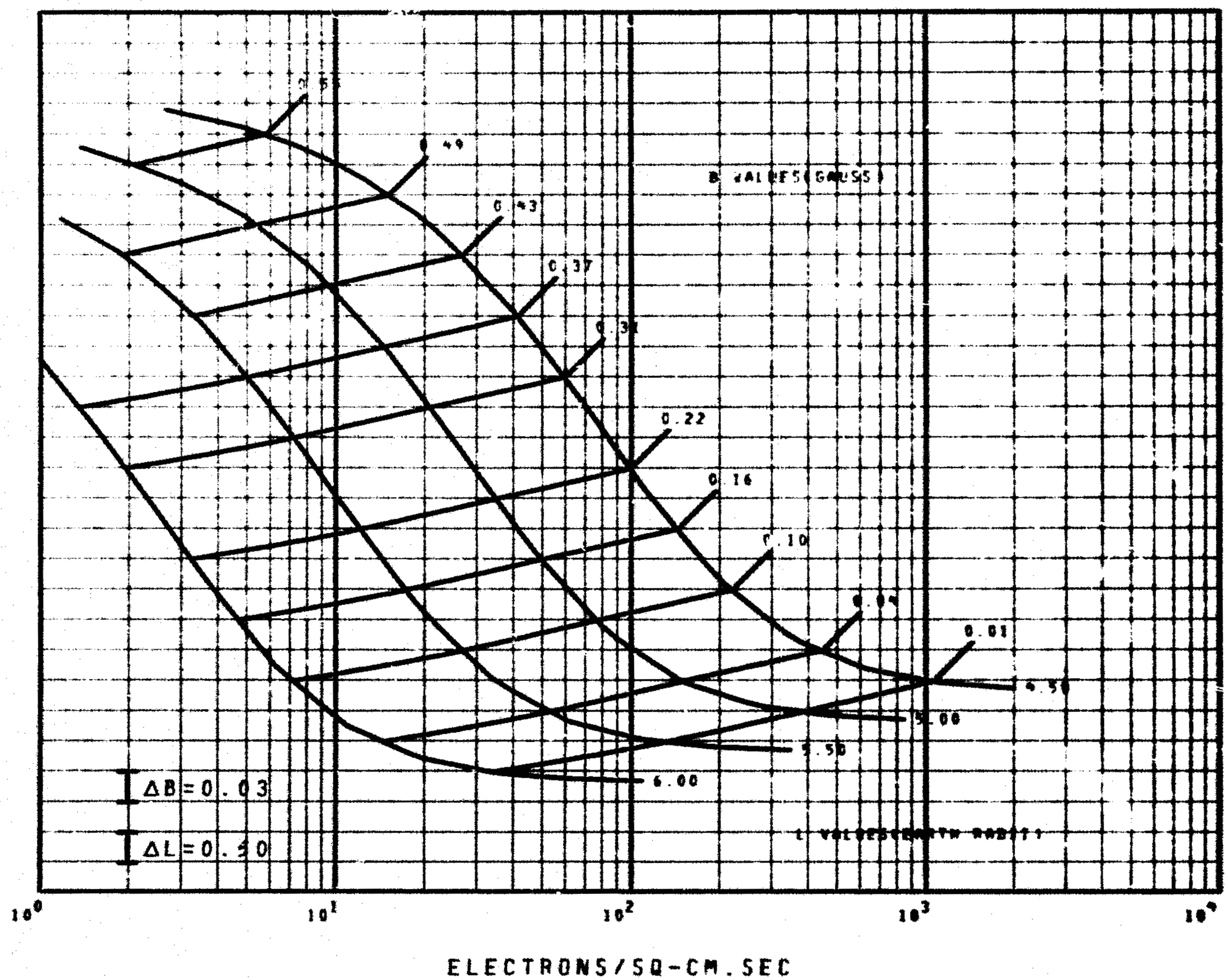

FIGURE 10 ORBITAL INTEGRATION MAP EPOCH 1980

CIRCULAR ORBIT 0 DEG INCLINATION

SOLAR MAXIMUM AE4 AND AE6 MODELS

(300 to 4000 n.m.)

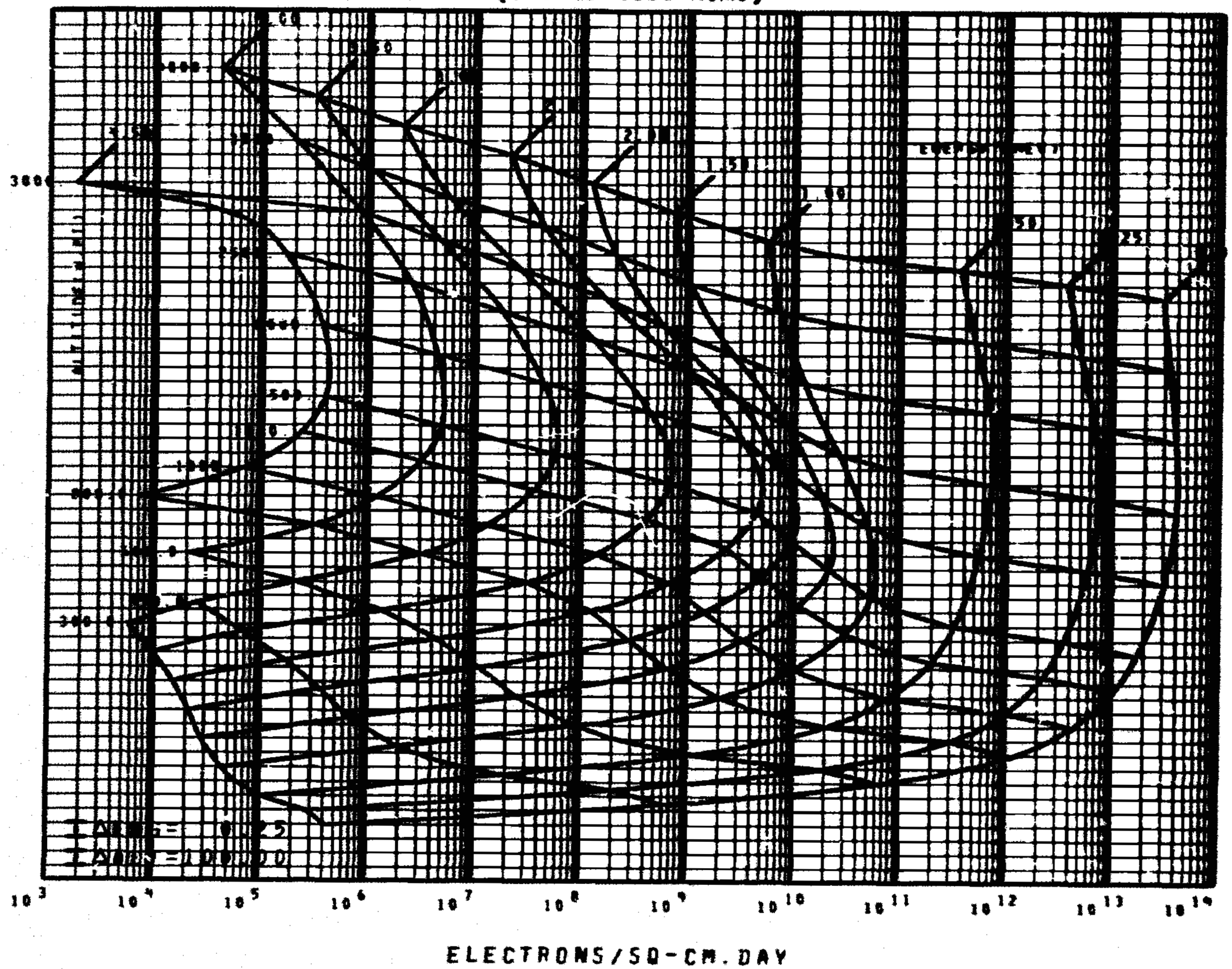

FIGURE 11 ORBITAL INTEGRATION MAP EPOCH 1980

CIRCULAR ORBIT 0 DEG INCLINATION

SOLAR MAXIMUM AE4 AND AE6 MODELS

(500 to 18,000 n.m.)

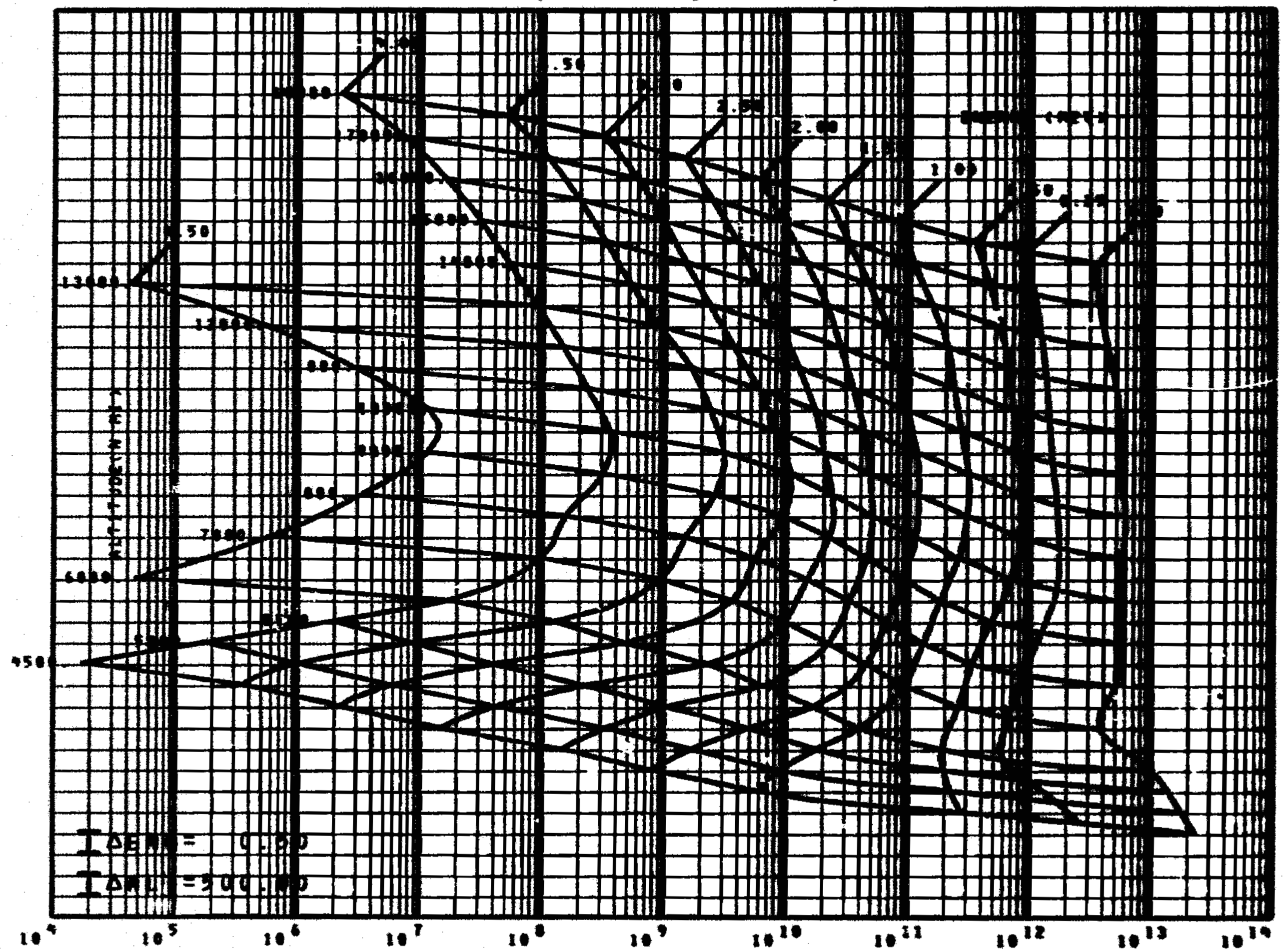

ELECTRONS/SQ-CM.DAY

FIGURE 12 ORBITAL INTEGRATION MAP EPOCH 1980

CIRCULAR ORBIT 30 DEG INCLINATION

SOLAR MAXIMUM AE4 AND AE6 MODELS

(150 to 4000 n.m.)

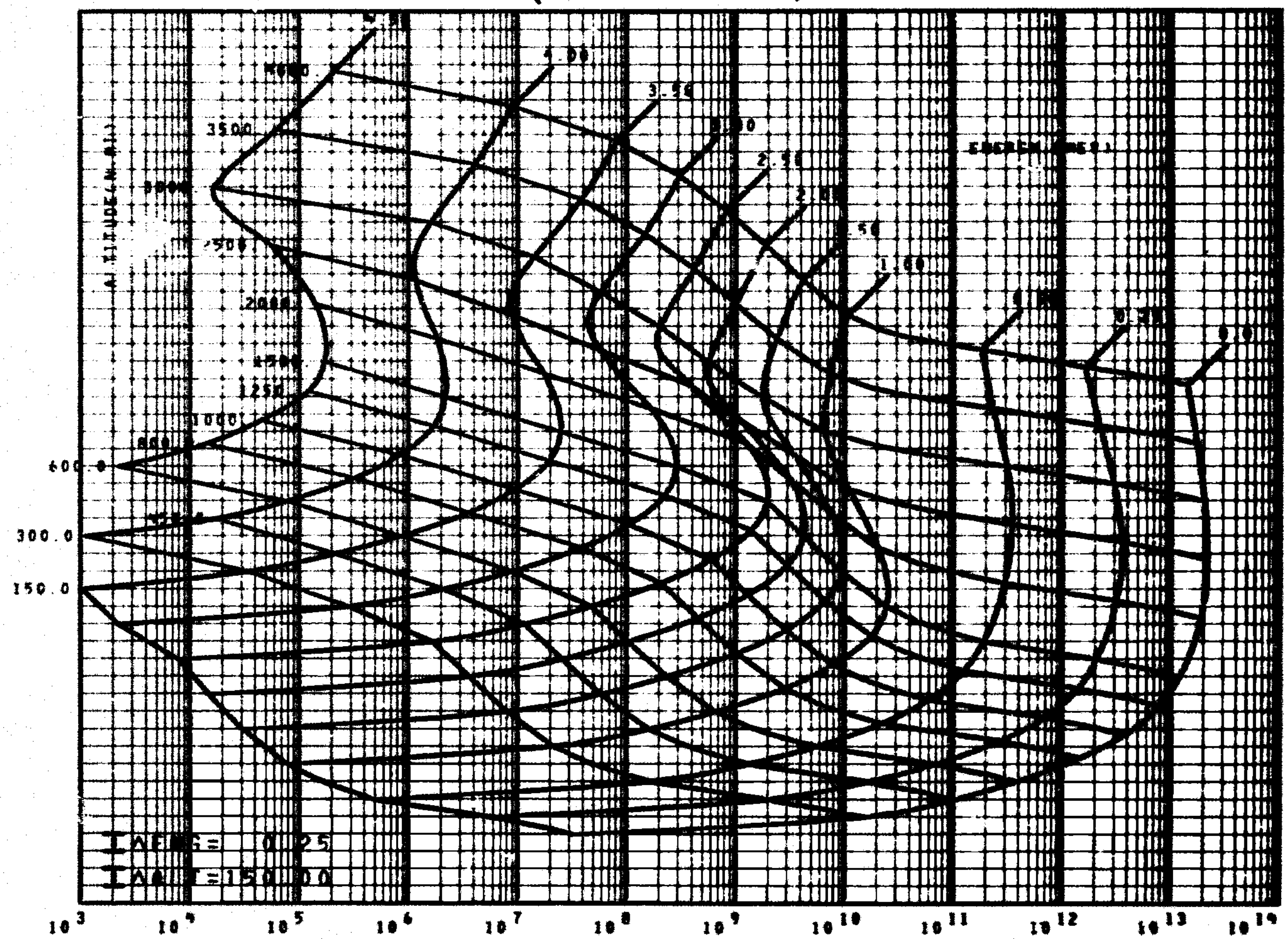

FIGURE 13 ORBITAL INTEGRATION MAP EPOCH 1980

CIRCULAR ORBIT 30 DEG INCLINATION

SOLAR MAXIMUM AE4 AND AE6 MODELS

(4,500 to 18,000 n.m.)

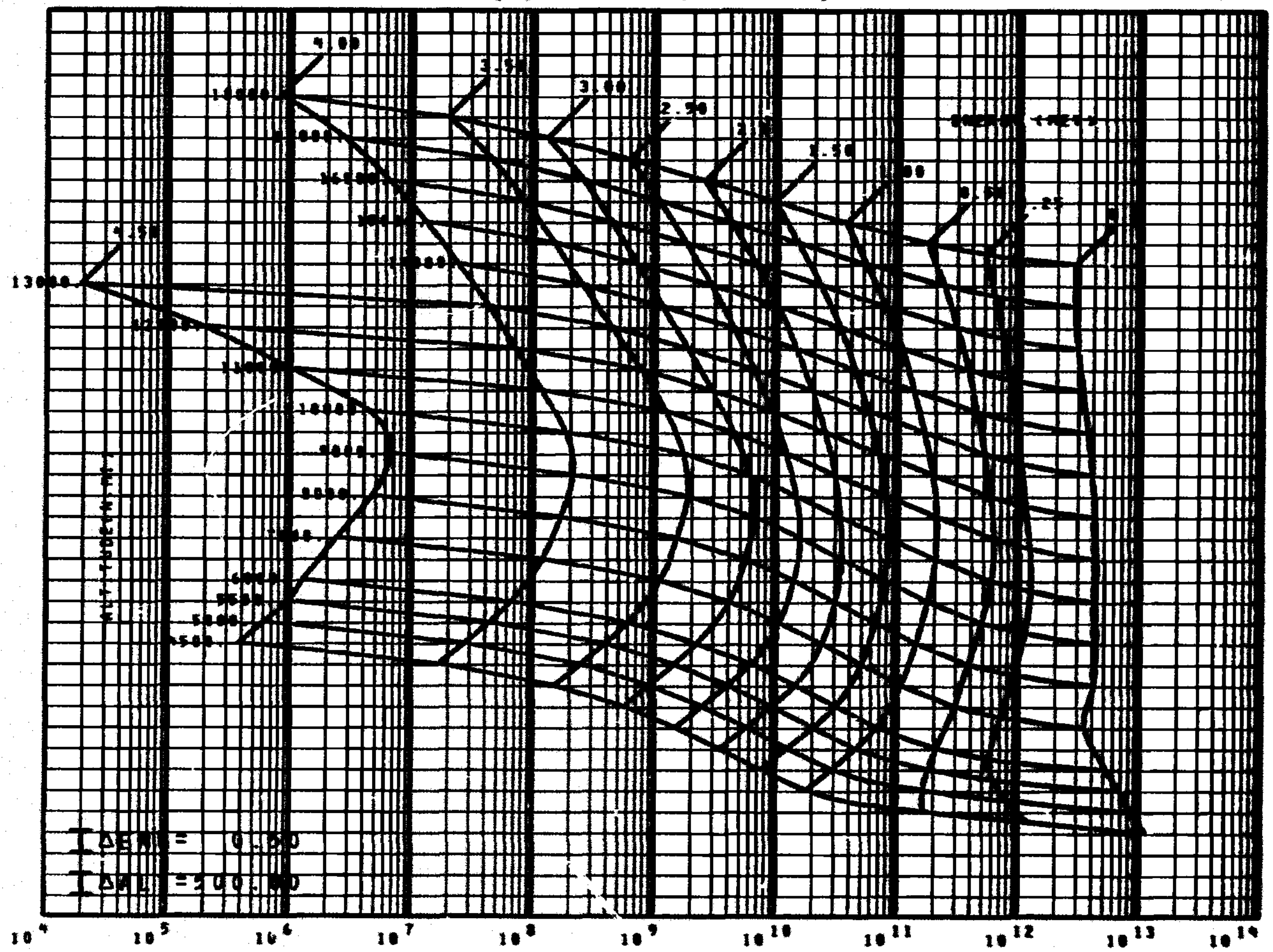

FIGURE 14 ORBITAL INTEGRATION MAP EPOCH 1980

CIRCULAR ORBIT 60 DEG INCLINATION

SOLAR MAXIMUM AE4 AND AE6 MODELS

(150 to 4000 n.m.)

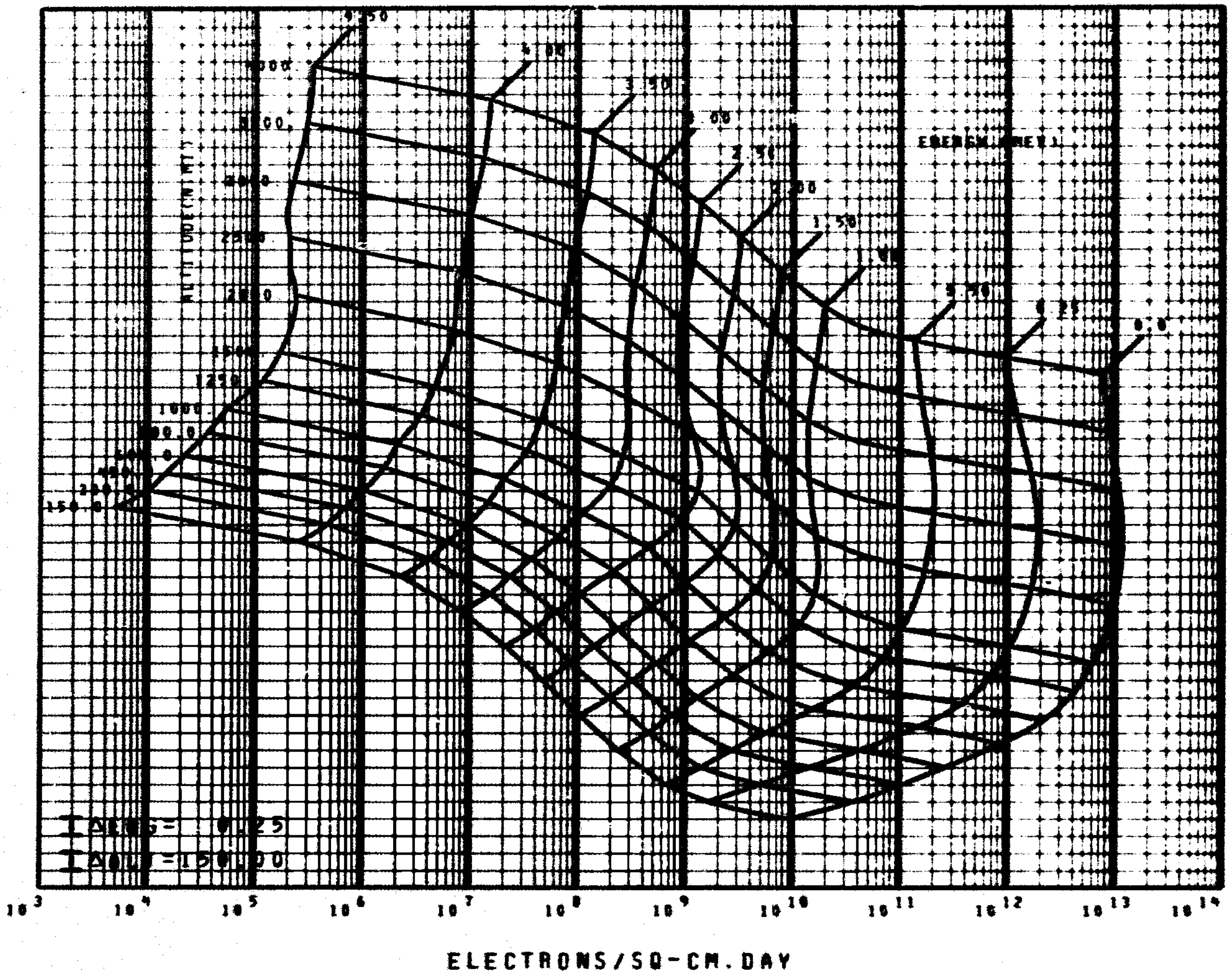

FIGURE 15 ORBITAL INTEGRATION MAP EPOCH 1980

CIRCULAR ORBIT 60 DEG INCLINATION

SOLAR MAXIMUM AE4 AND AE6 MODELS

(4,500 to 18,000 n.m.)

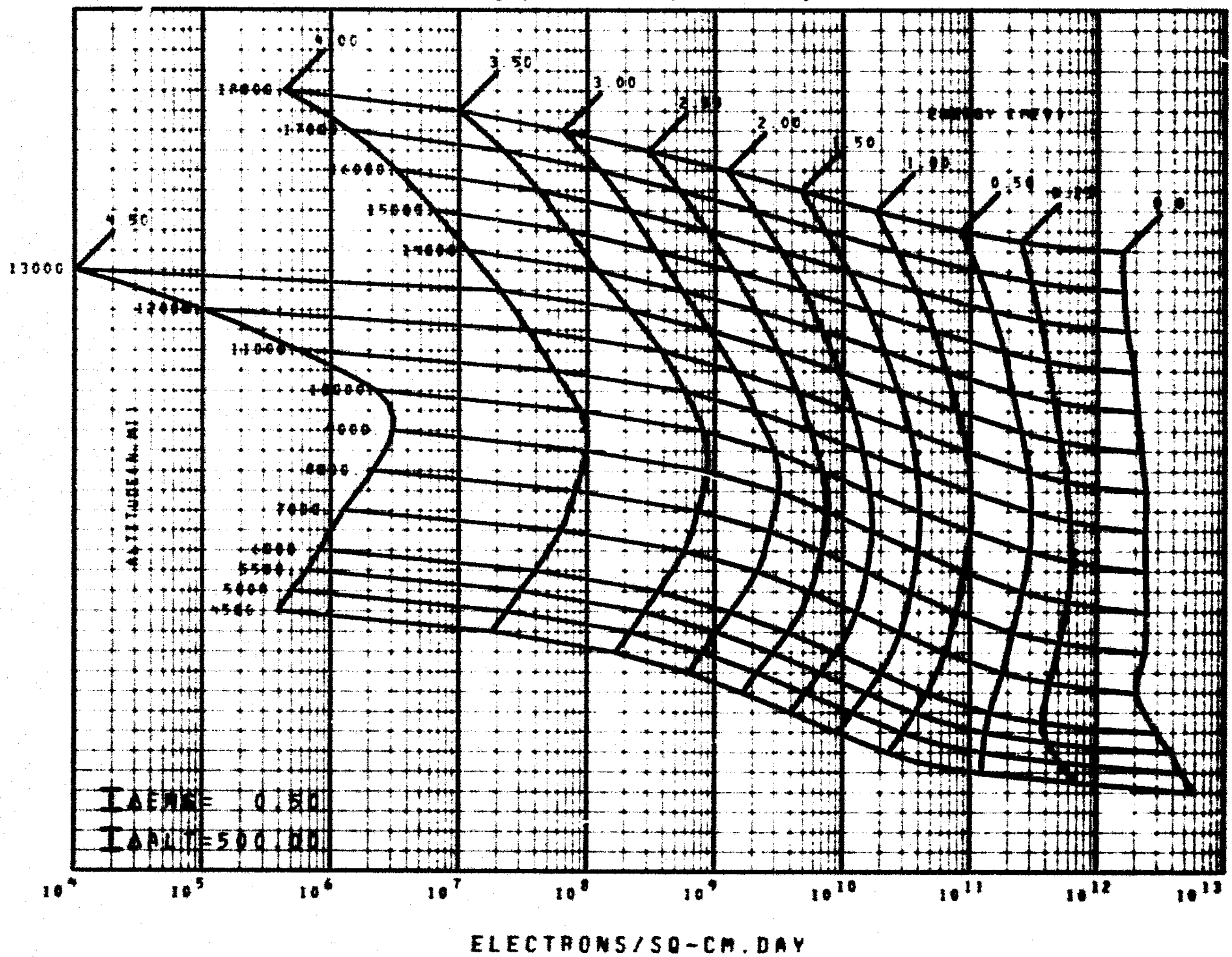

FIGURE 16 ORBITAL INTEGRATION MAP EPOCH 1980

CIRCULAR ORBIT 90 DEG INCLINATION

SOLAR MAXIMUM AE4 AND AE6 MODELS

(150 to 4000 n.m.)

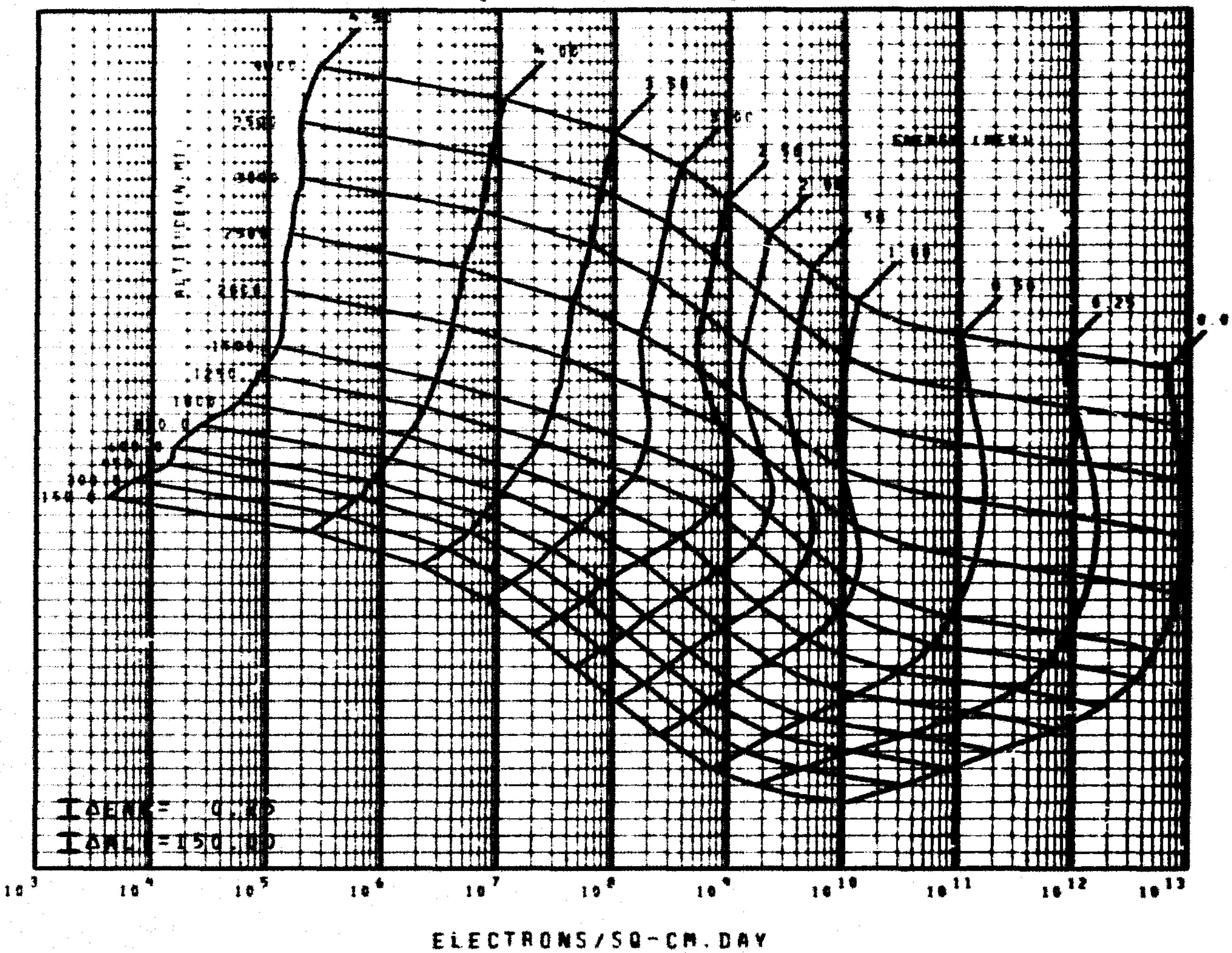

FIGURE 17 ORBITAL INTEGRATION MAP EPOCH 1980

CIRCULAR ORBIT 90 DEG INCLINATION

SOLAR MAXIMUM AE4 AND AE6 MODELS

(4,500 to 18,000 n.m.)

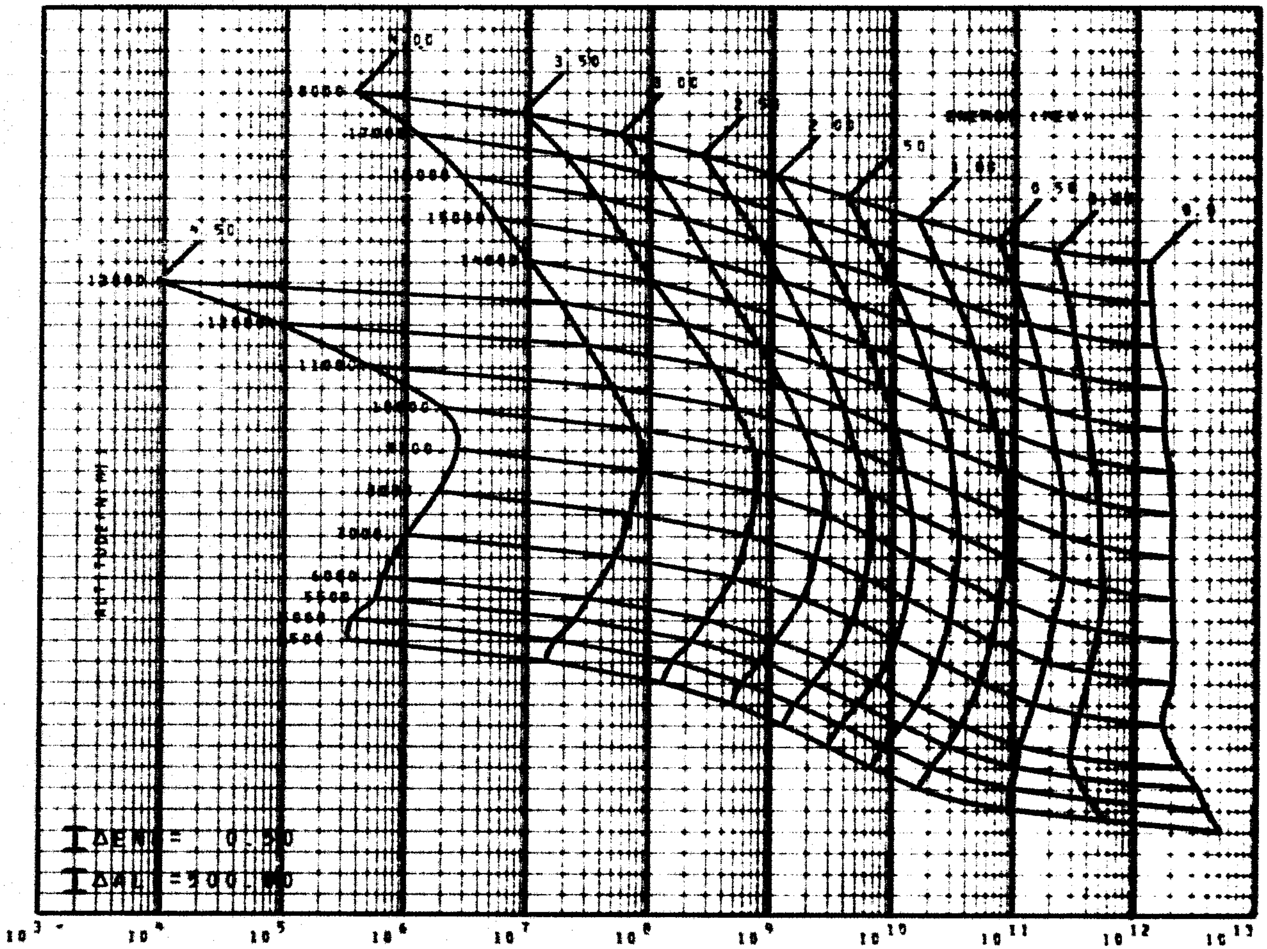

ELECTRONS/SQ-CM.DAY

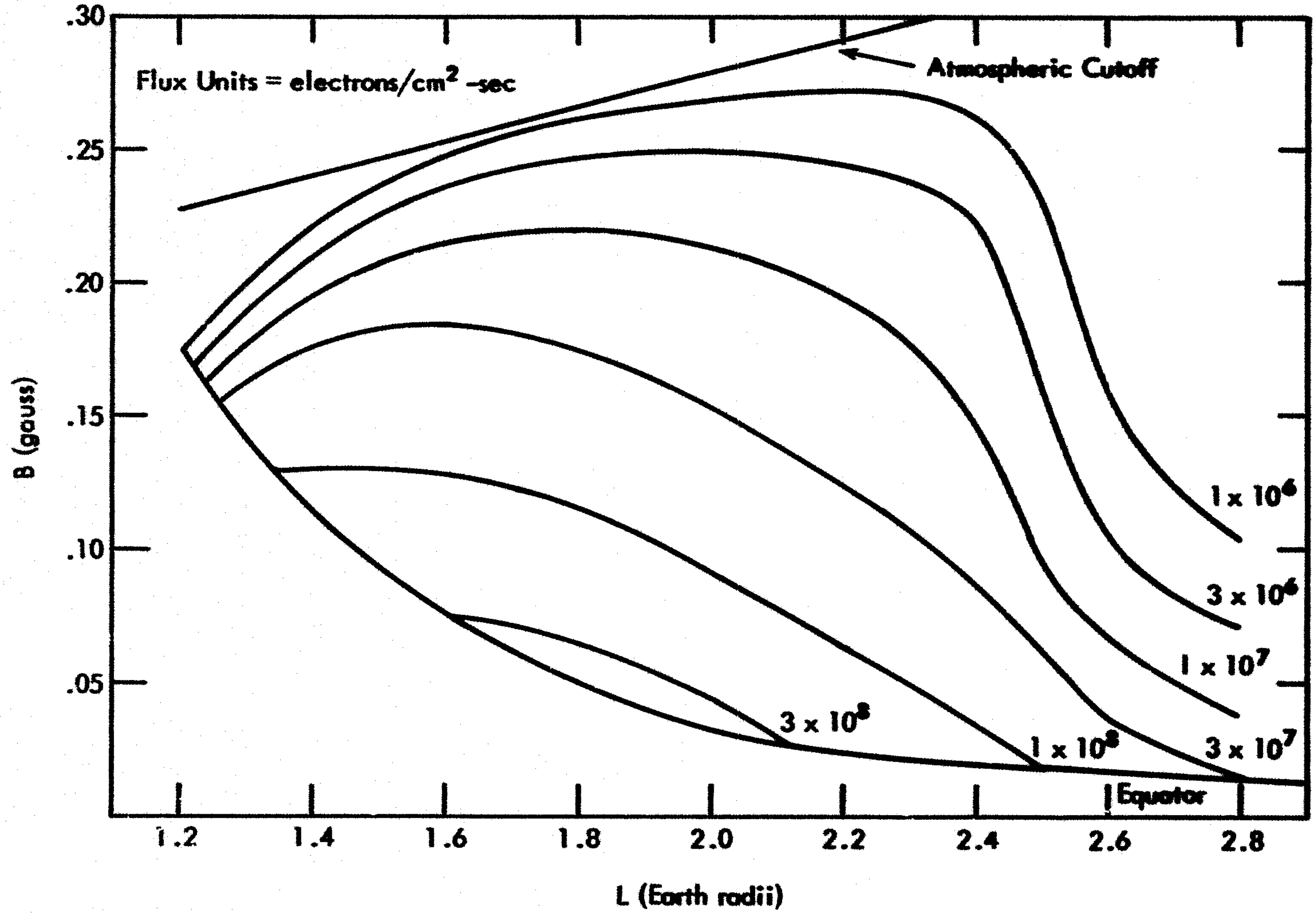

Figure 18. B–L Projection of AE 6 Omnidirectional Iso-flux Contours for 40-kev Electrons

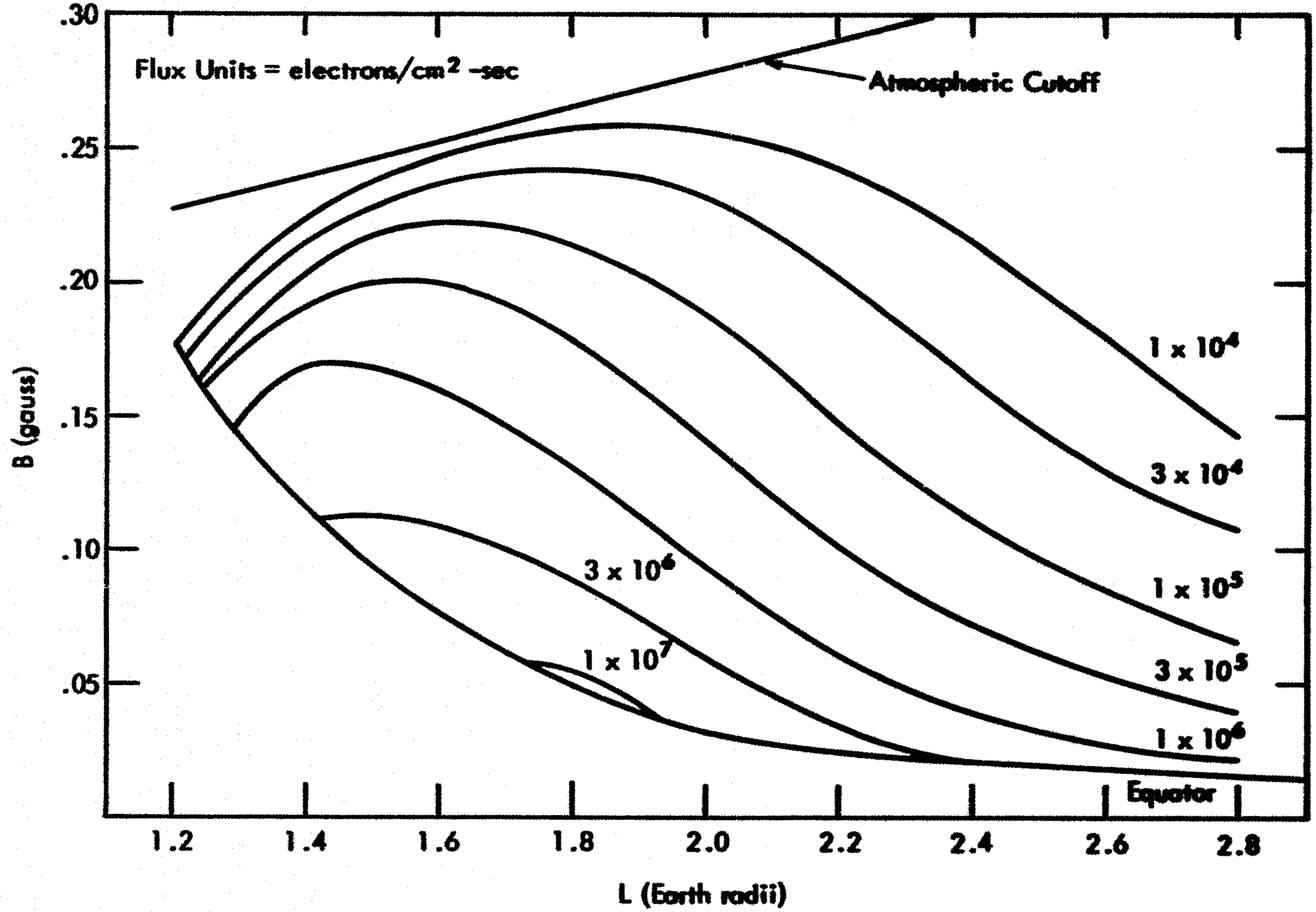

Figure 19. B–L Projection of AE 6 Omnidirectional Iso-flux Contours for 500-kev Electrons

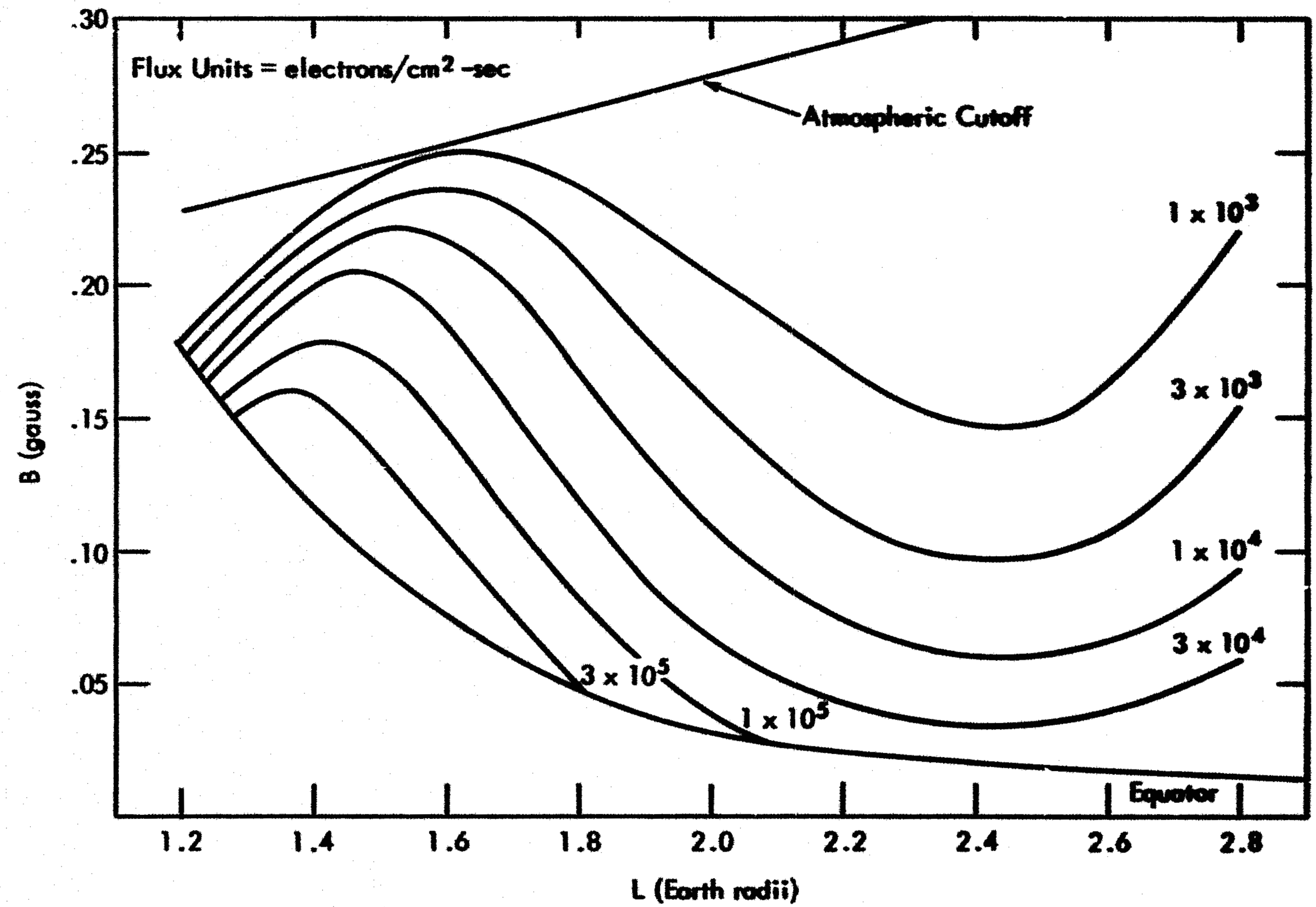

Figure 20. B–L Projection of AE 6 Omnidirectional Iso-flux Contours for 1-Mev Electrons

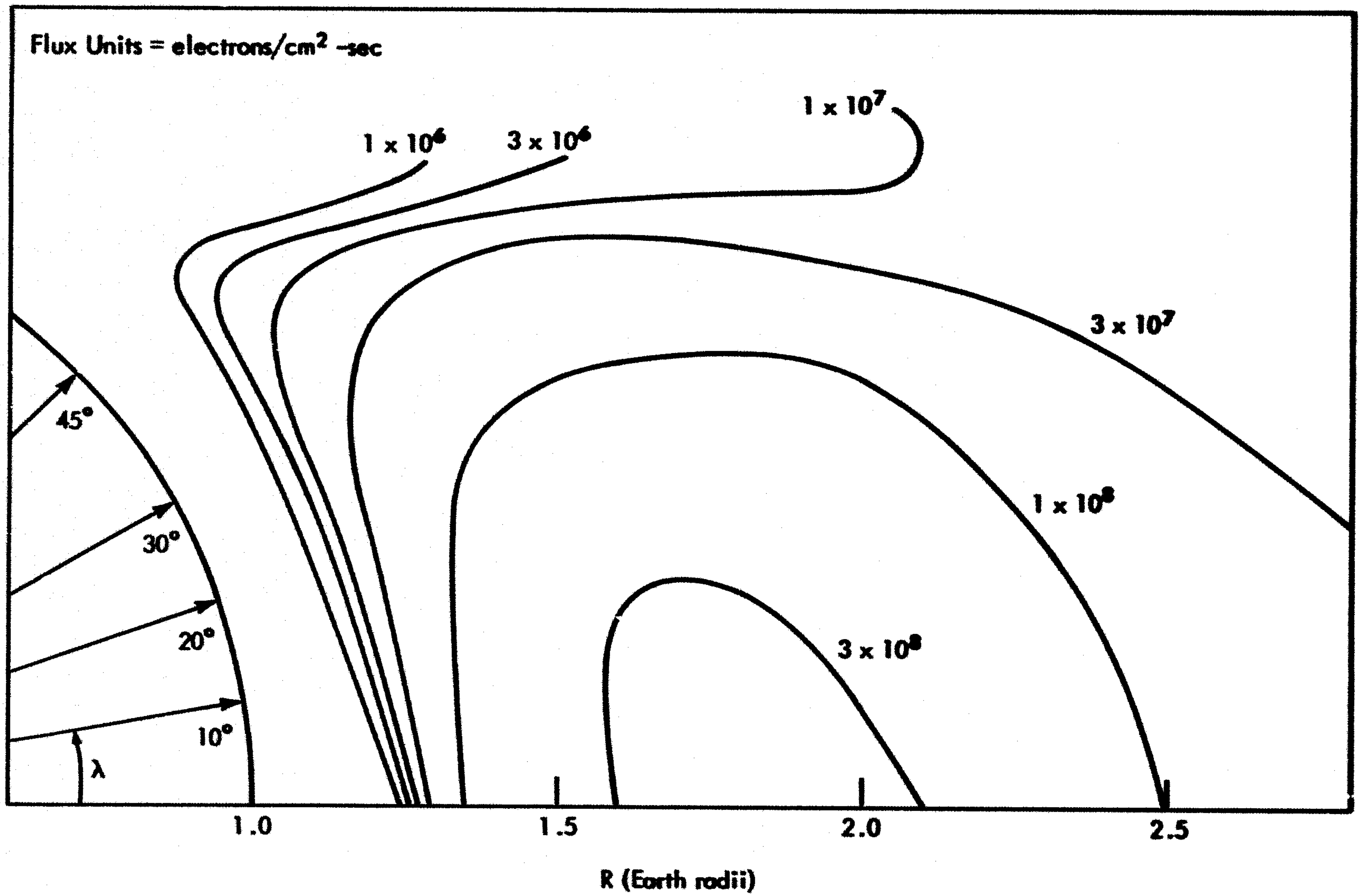

Figure 21. R–λ Projection of AE 6 Omnidirectional Iso-flux Contours for 40-kev Electrons

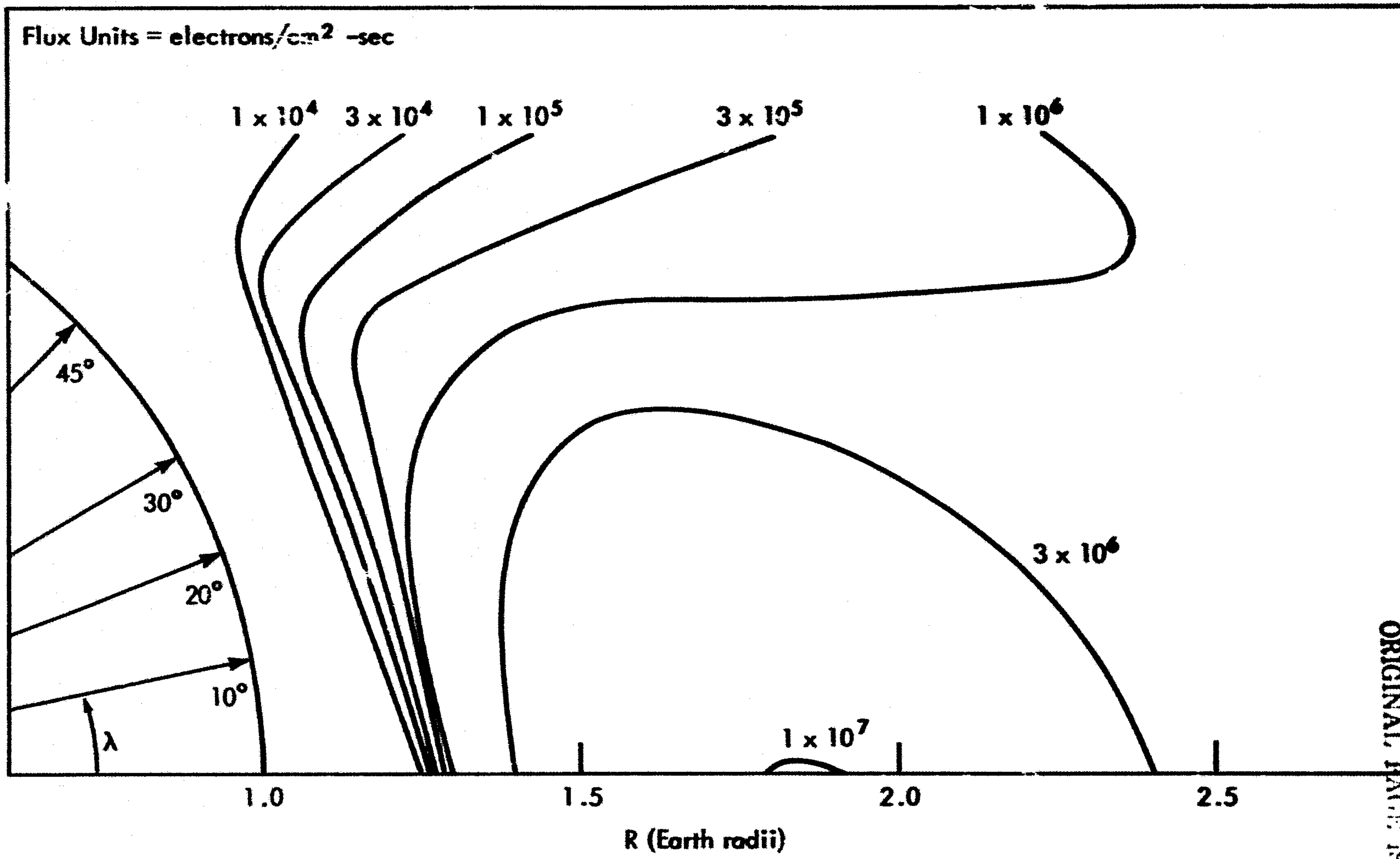

Figure 22. R-λ Projection of AE 6 Omnidirectional Iso-flux Contours for 500-kev Electrons

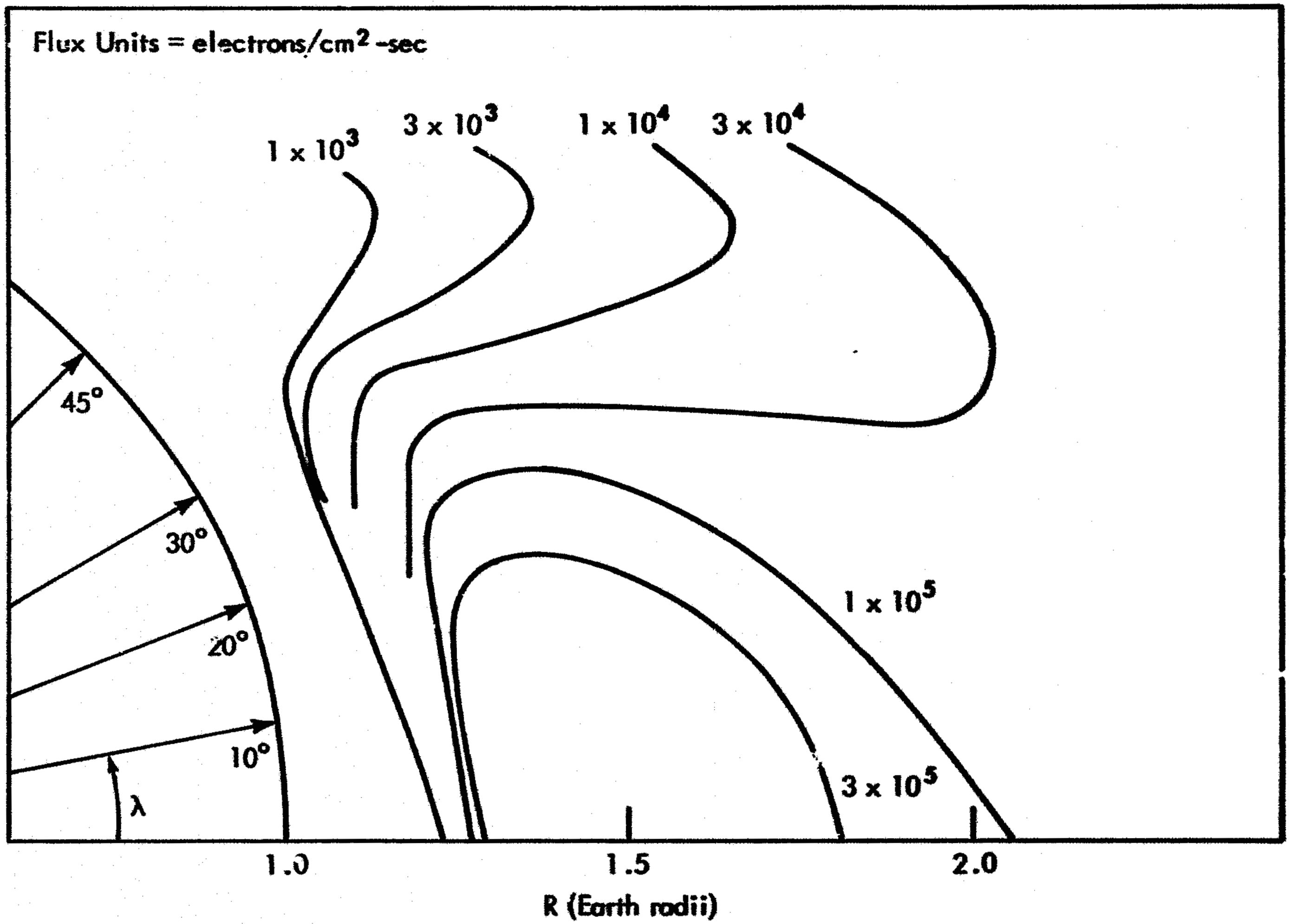

Figure 23. R-λ Projection of AE 6 Omnidirectional Iso-flux Contours for 1-Mev Electrons

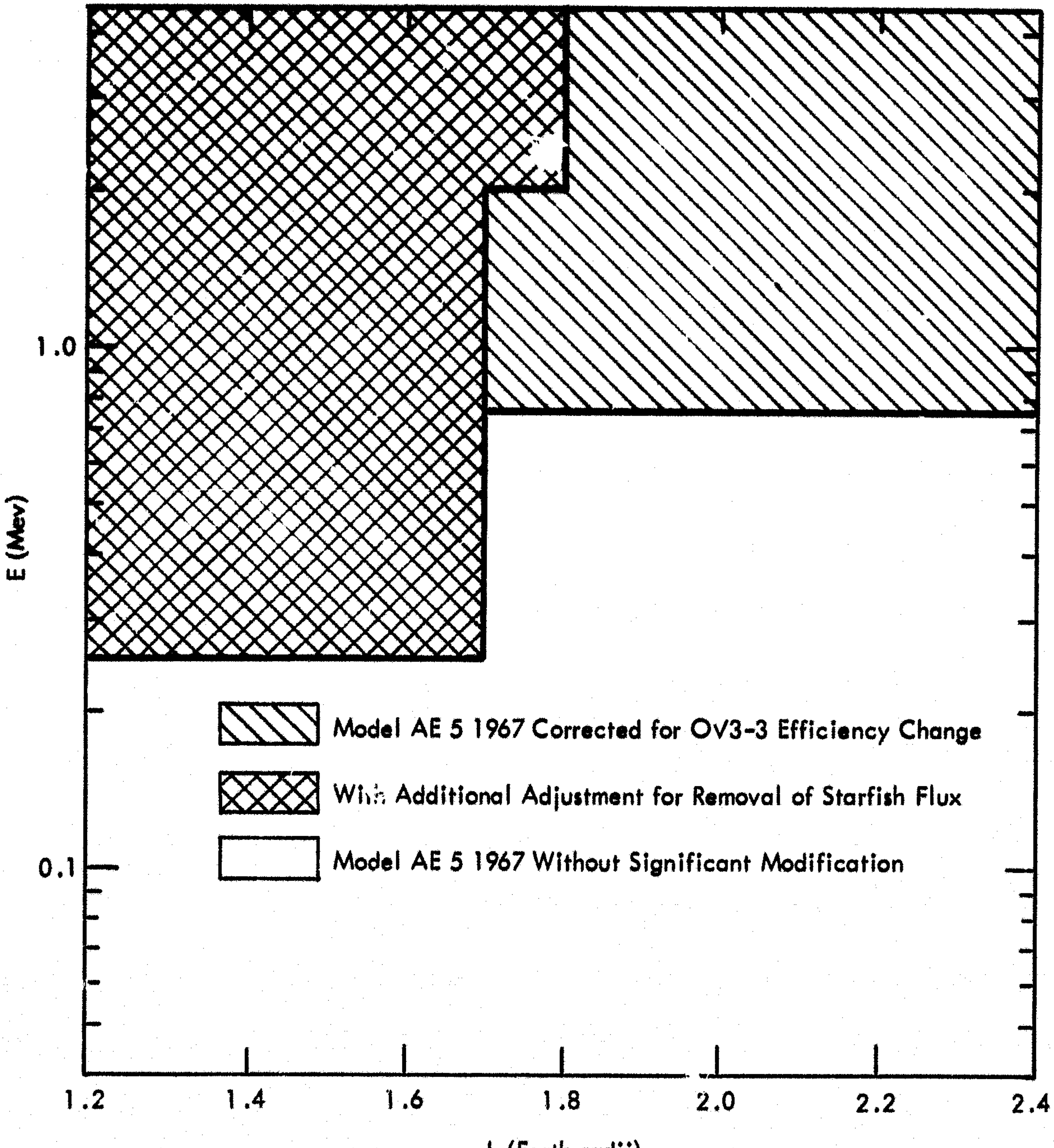

Figure 24. Derivation of the Model AE 6

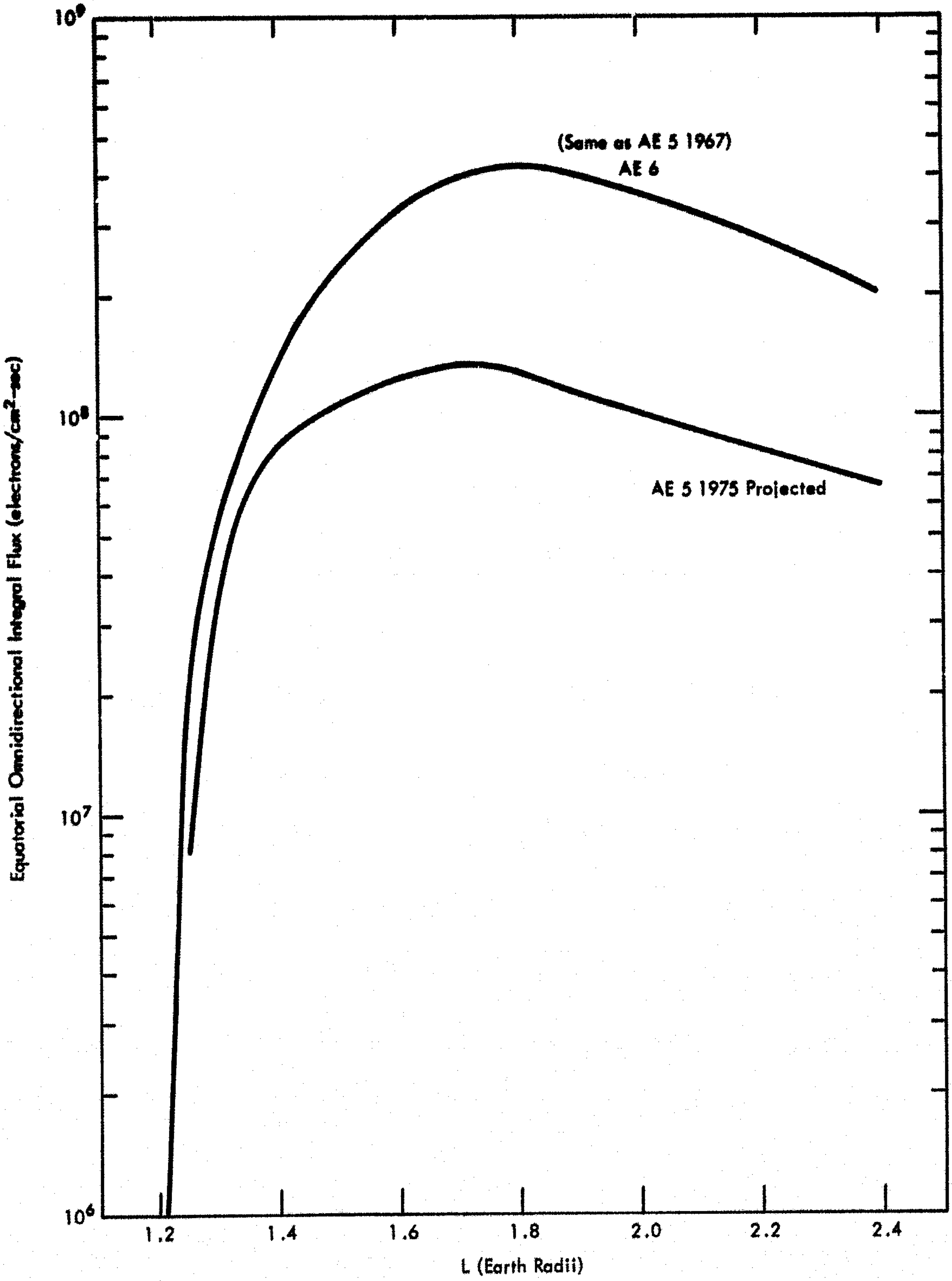

Figure 25. Inner Zone Radial Profile for 40-kev Electrons

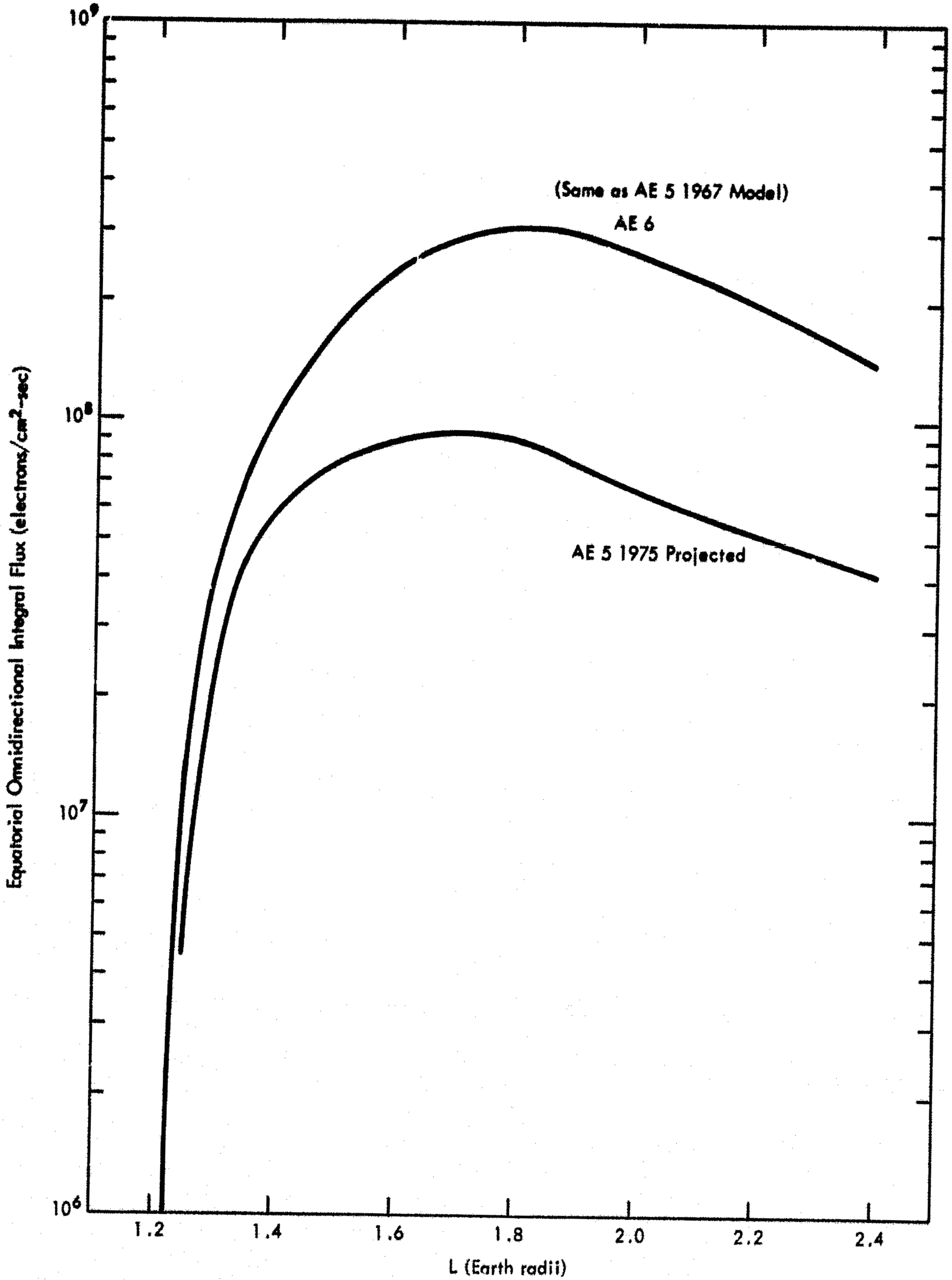

Figure 26. Inner Zone Radial Profile for 100-kev Electrons

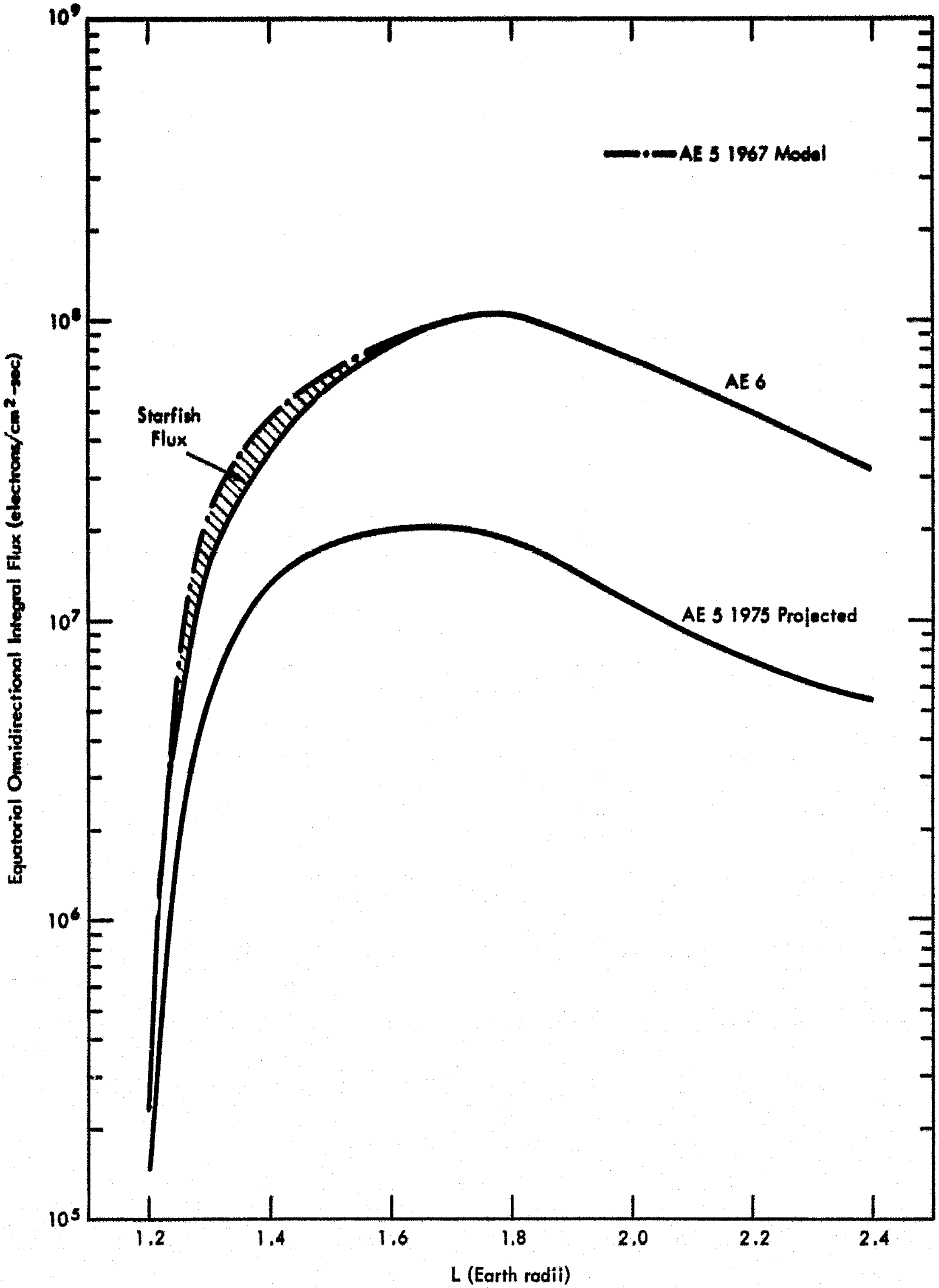

Figure 27. Inner Zone Radial Profile for 250-kev Electrons

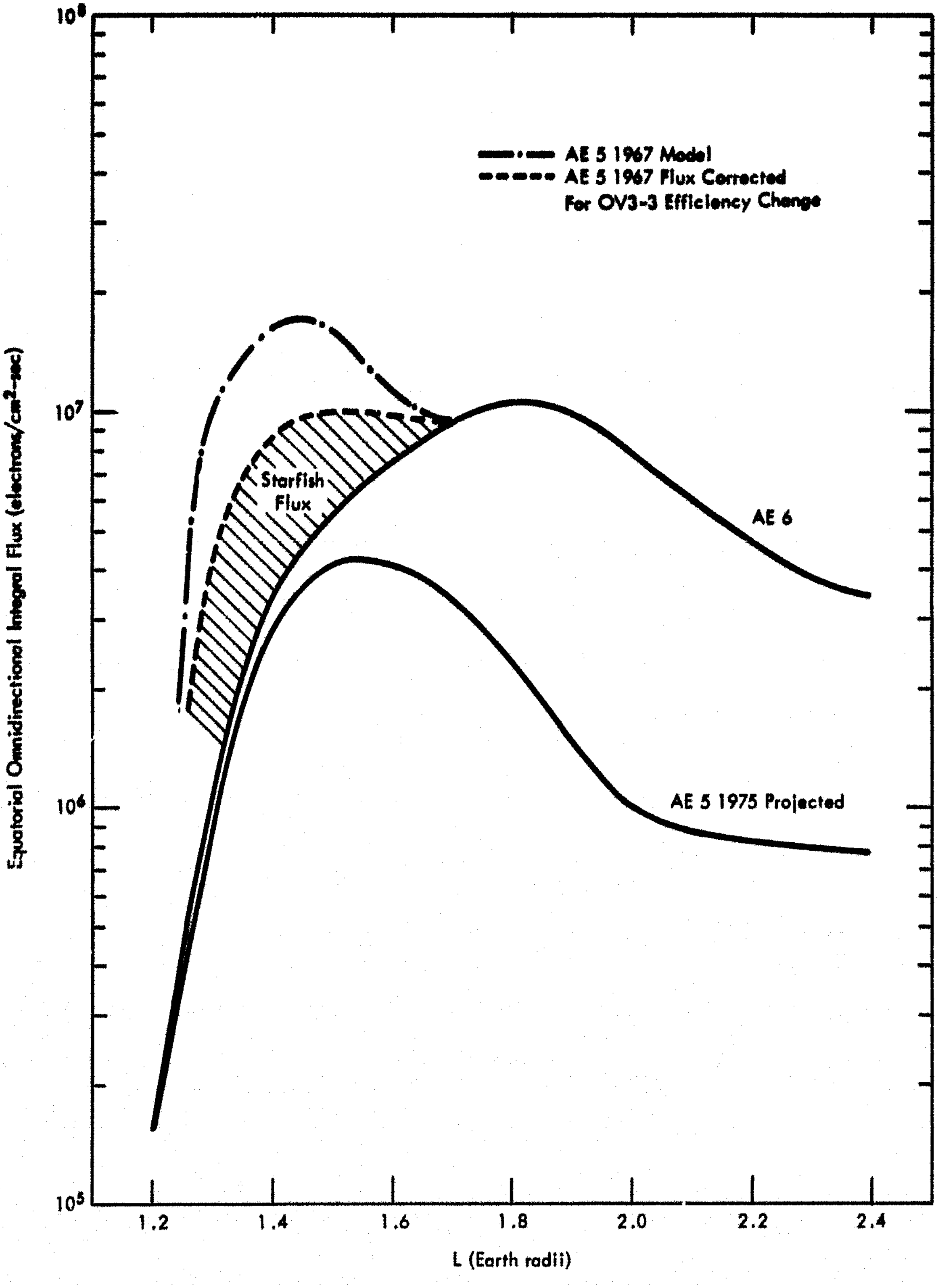

Figure 28. Inner Zone Radial Profile for 500-kev Electrons

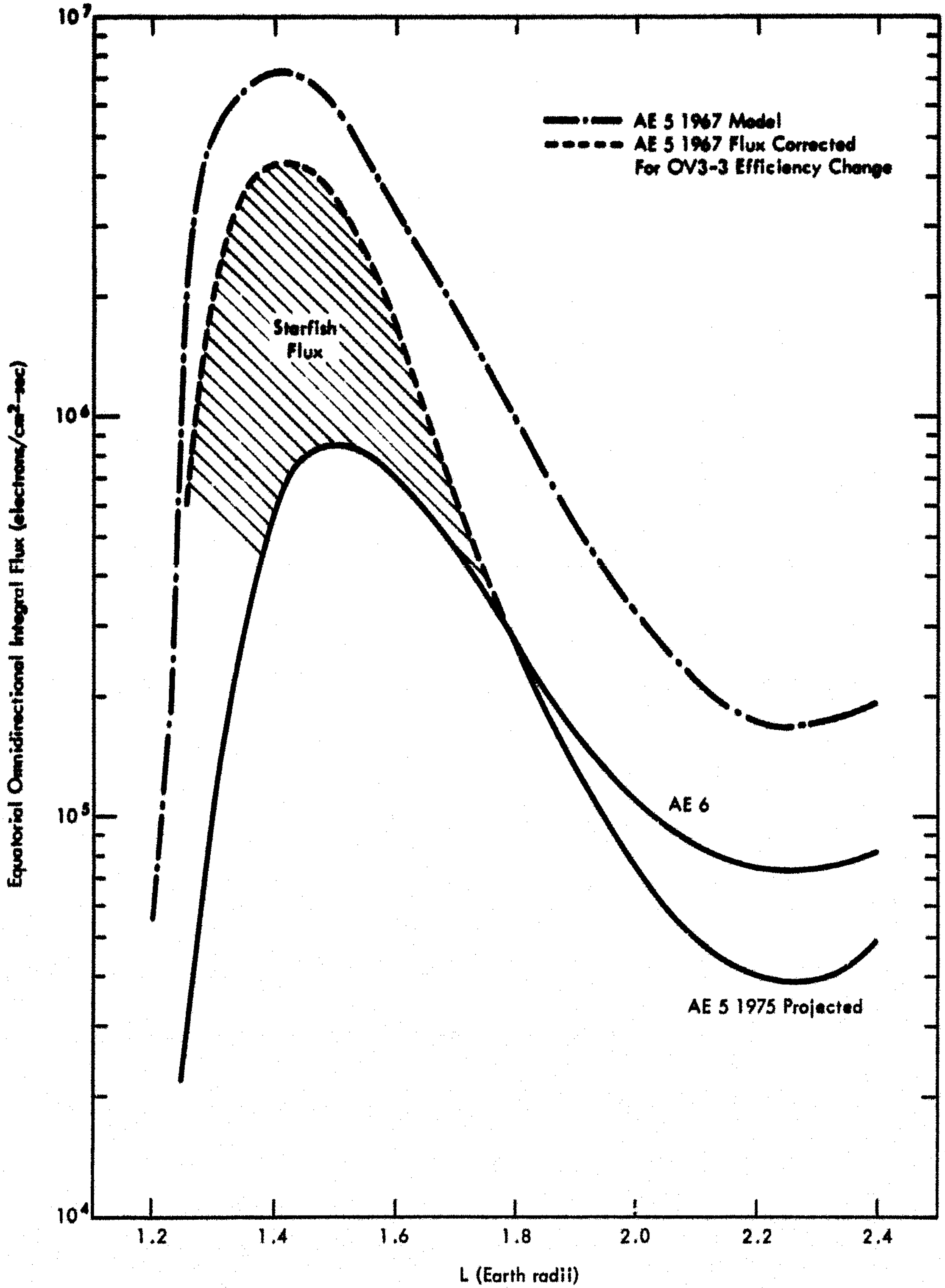

Figure 29. Inner Zone Radial Profile for 1-Mev Electrons

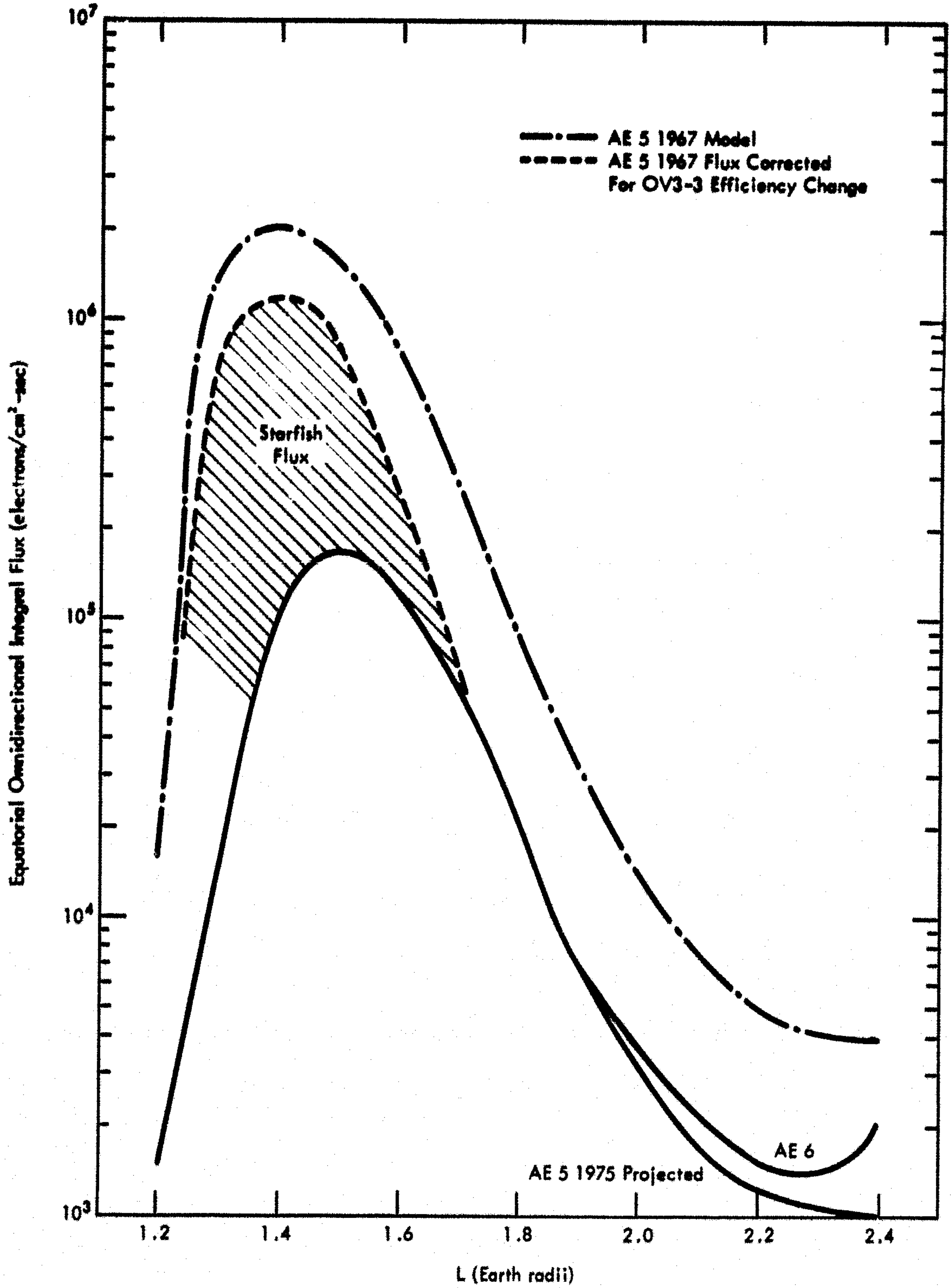

Figure 30. Inner Zone Radial Profile for 2-Mev Electrons

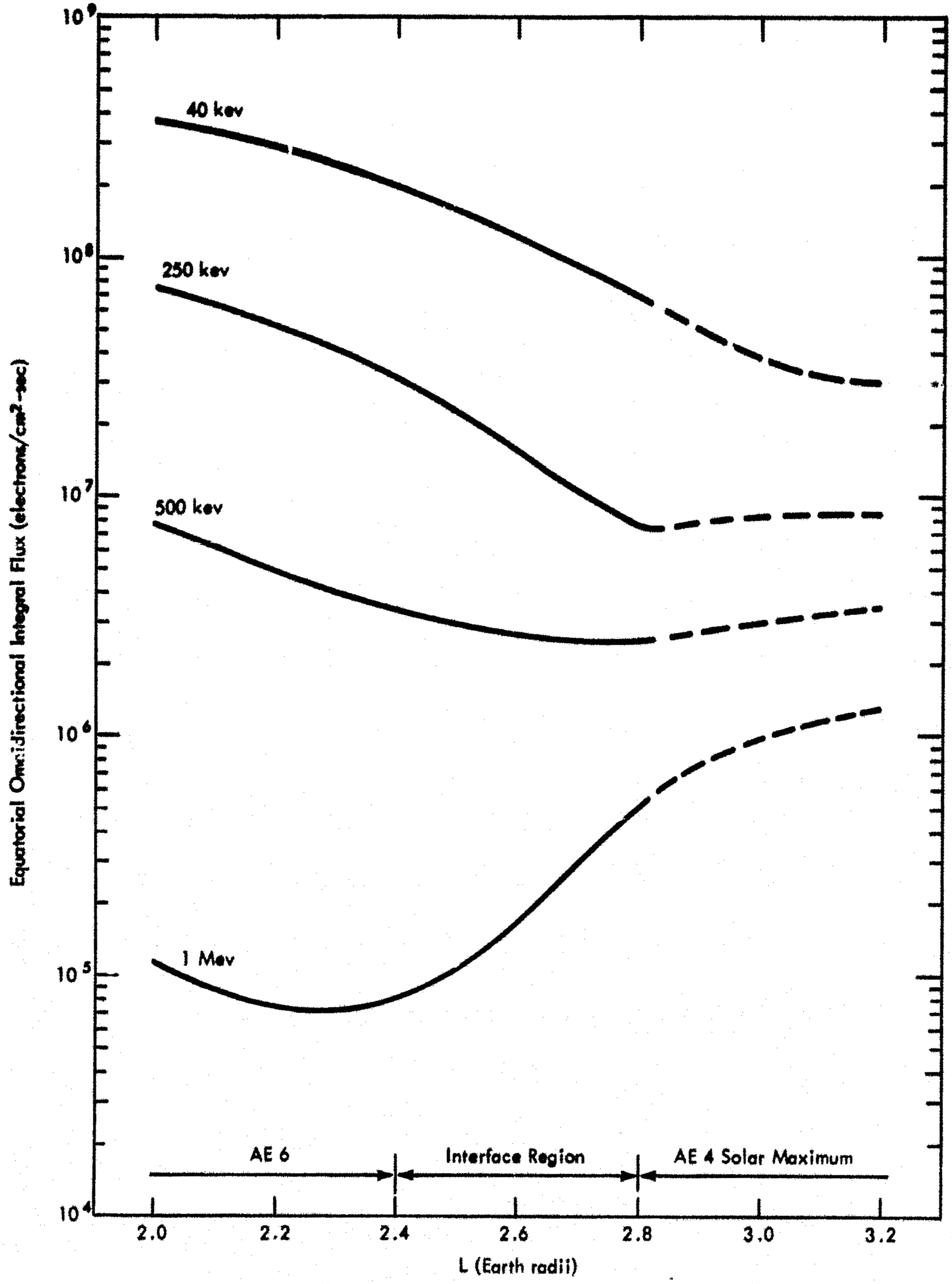

Figure 31. Radial Profile in Model-Interface Region (40 kev to 1.0 Mev)

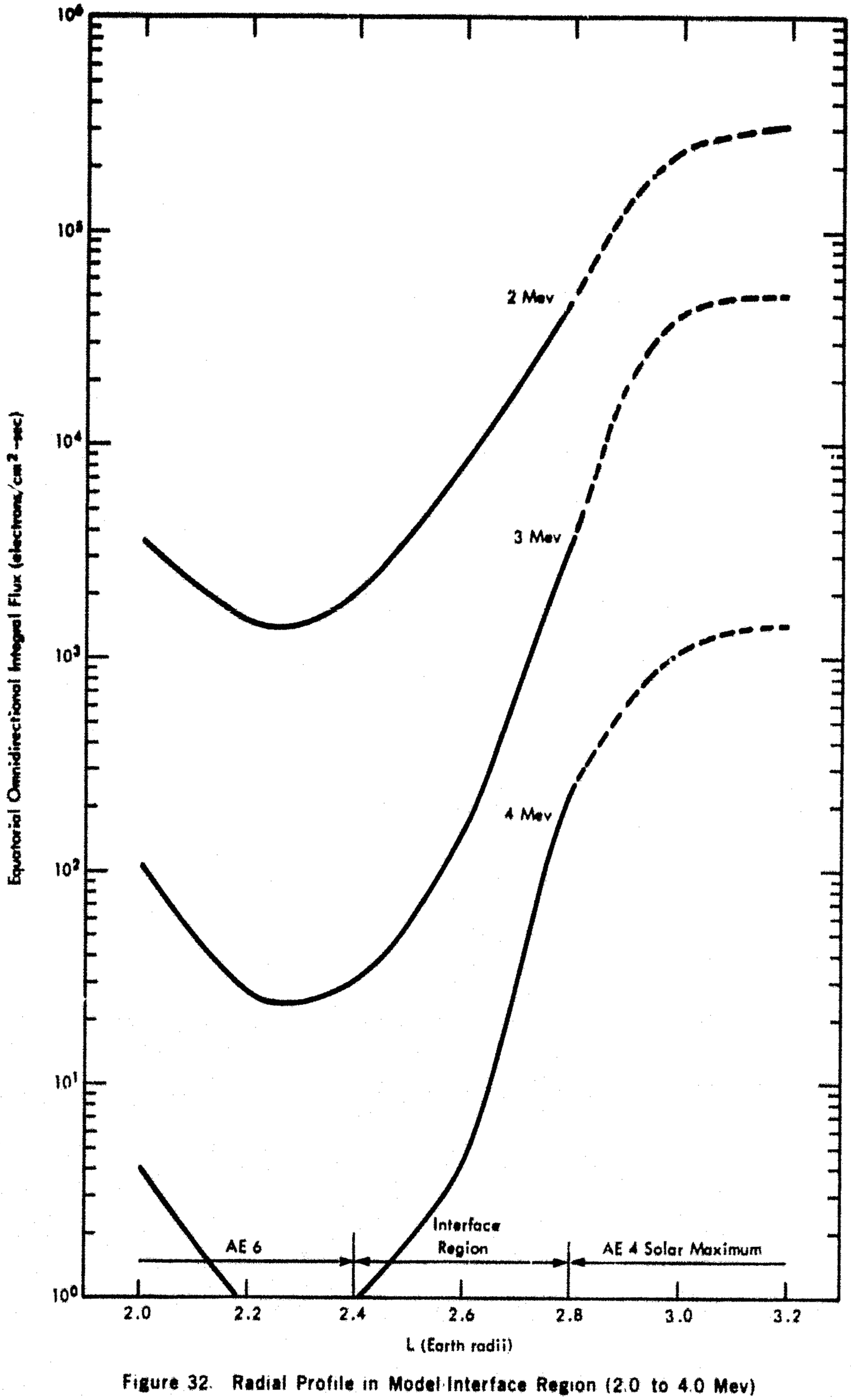

Figure 32. Radial Profile in Model-Interface Region (2.0 to 4.0 Mev)